Extracting Quantum Entanglement

via Quantum Monte Carlo:

human

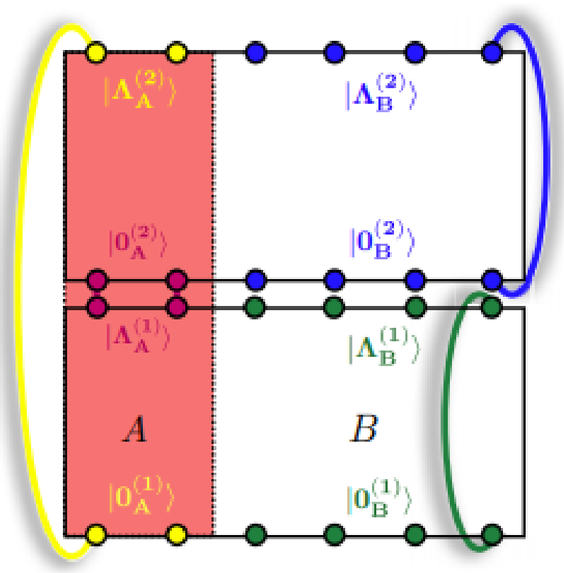

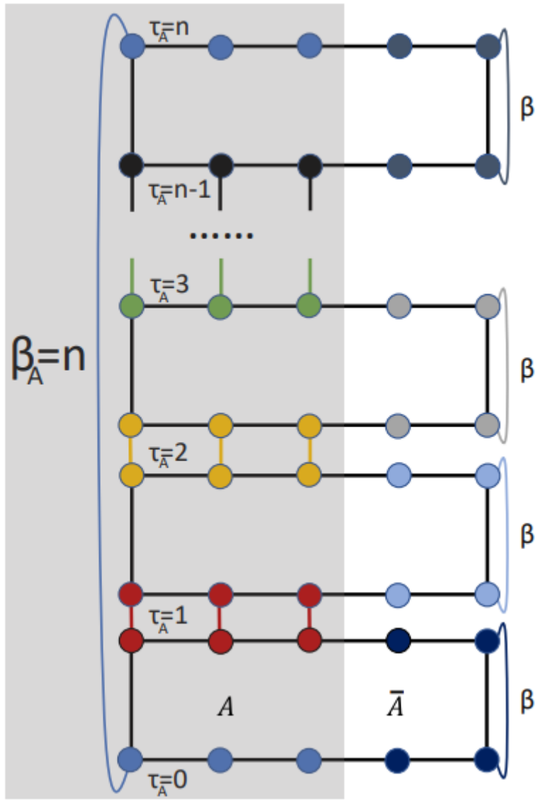

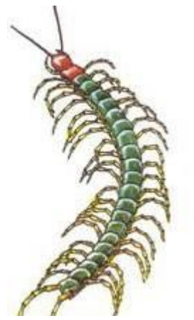

chilopod

西湖大學 WESTLAKE UNIVERSITY

Zheng YAN (严正)

Westlake University

0 What's quantum entanglement?

$|A, \bar{A}\rangle$ *can not be written as* $|A\rangle \otimes |\bar{A}\rangle$

1 What is entanglement entropy?

Entanglement entropy is defined via density matrix ρ. For a pure quantum state $|\Psi\rangle$,

$$\rho = |\Psi\rangle\langle\Psi|$$

1. von-Neumann entropy: $S_A^{(vN)} = -\operatorname{Tr}_A \rho_A \ln \rho_A$
   - $\rho_A = \operatorname{Tr}_B \rho$
   - calculation requires wave function
   - DMRG is successful in 1D, but limited in 2D systems

2. Rényi entropy: $S_A^{(n)} = -\frac{1}{n-1} \ln \left[\operatorname{Tr}_A \left(\rho_A^n\right)\right] = -\frac{1}{n-1} \ln \left[\frac{Z_A^{(n)}}{Z^{(n)}}\right]$[1]
   - $n \to 1$, Rényi entropy converges to von-Neumann entropy.
   - $Z^{(2)} = \sum_{n_A, m_A, n_B, m_B} < n_A n_B \left| e^{-\beta H} \right| n_A n_B >< m_A m_B \left| e^{-\beta H} \right| m_A m_B >$
   - $Z_A^{(2)} = \sum_{n_A, m_A, n_B, m_B} < n_A n_B \left| e^{-\beta H} \right| m_A n_B >< m_A n_B \left| e^{-\beta H} \right| n_A n_B >$
   - n-th Rényi entropy is obtainable in QMC!

2 What can entanglement entropy do?

Scaing of the entanglement entropy:

- For a free scalar bosonic field: $S_A^n = a_n L^{d-1} + \cdots$
- Corrections to area law are universal.
- Can be used to classify quantum phases and quantum phase transitions, and detect topological order

Physical state	Entropy	Example
d=1 CFT	$\frac{c}{3} \ln L$	$s = \frac{1}{2}$ Heisenberg chain
$d \geq 2$ QCP	$aL^{d-1} + \gamma_{\text{QCP}}$	Wilson-Fisher O(N)
Ordered (brok. cont. sym.)	$aL^{d-1} + \frac{n_G}{2} \ln L$	Superfluid, Néel order
Gapped (brok. disc. sym.)	$aL^{d-1} + \ln(\text{deg})$	Gapped XXZ
Topological order	$aL^{d-1} - \gamma_{\text{top}}$	$\mathcal{Z}_2$ spin liquid

Table 1: scaling form for various states of matter[2]

Exception to the are law: $d > 1$ fermions
For conventional metals with a well defined Fermi surface,

$$S_A^n = \text{Area law} \times \ln(L^{d-1}) + \cdots$$

[2] **Laflorencie, N., *Phys. Rep.*, *646*, 1-59 (2016).**

3 Numerical advancement

3.1 Measurement at finite temperature

Way 1:

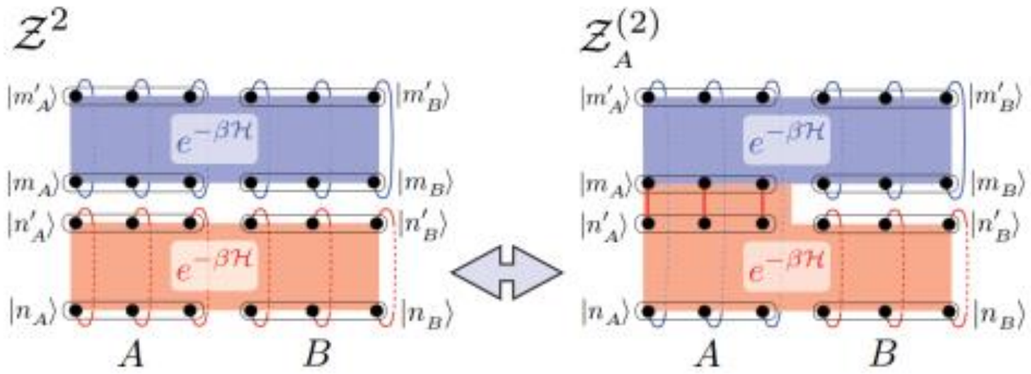

$$Z^{(2)} = \sum_{n_A,m_A,n_B,m_B} < n_A n_B \left| e^{-\beta H} \right| n_A n_B >< m_A m_B \left| e^{-\beta H} \right| m_A m_B >$$

$$Z_A^{(2)} = \sum_{n_A,m_A,n_B,m_B} < n_A n_B \left| e^{-\beta H} \right| m_A n_B >< m_A n_B \left| e^{-\beta H} \right| n_A n_B >$$

Extended ensemble[3]: $Z^{(2)} \cup Z_A^{(2)}$

- $P\left(\mathcal{Z}^2 \to \mathcal{Z}_A^{(2)}\right) = \min\left[1, w_A(\mathcal{C})/w_{A=\varnothing}(\mathcal{C})\right]$
- $\frac{Z_A^{(2)}}{Z^{(2)}} = \langle N_A/N_{A=\varnothing} \rangle_{\mathrm{MC}}$

[3] Humeniuk, S., & Roscilde, T. *Phys. Rev. B*, *86*, 235116 (2012) .

Way 2:

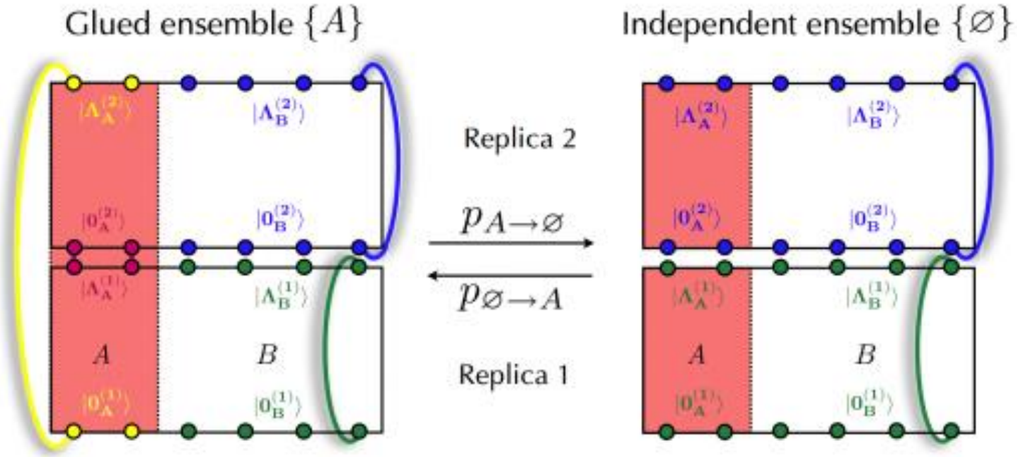

Alternative way[4]:

- Master equation: $\frac{\mathrm{d}P_A(t)}{\mathrm{d}t} = P_\varnothing(t)p_{\varnothing\to A} - P_A(t)p_{A\to\varnothing}$
- Equilibrium: $\frac{P_A}{P_\varnothing} = \frac{p_{\varnothing\to A}}{p_{A\to\varnothing}}$
- $S_A^{(n)} = \frac{1}{1-n}\ln\left(\frac{p_{\varnothing\to A}}{p_{A\to\varnothing}}\right)$
- $p_{\varnothing\to A} = \frac{N_{\text{satisfying both BCs}}}{N_{tot}}$, $p_{A\to\varnothing} = \frac{N_{\text{satisfying both BCs}}}{N_{tot}}$

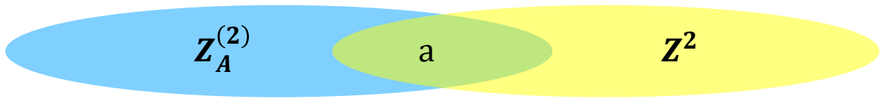

$$\frac{Z_A^{(2)}}{Z^2} = \frac{Z_A^{(2)}}{a}\frac{a}{Z^2}$$

[4] Luitz, D. J., Plat, X., Laflorencie, N., & Alet, F. *Phys. Rev. B*, *90*, 125105 (2014).

Comments on the above methods:

1. $S_A^{(2)} = \frac{1}{1-n} \ln\left(\frac{p_{\varnothing \to A}}{p_{A \to \varnothing}}\right) = aL + \cdots$ is proportional to L
   - $S_A^{(2)} = 10$ means $\frac{p_{\varnothing \to A}}{p_{A \to \varnothing}} = 0.0000454$
   - $S_A^{(2)} = 12$ means $\frac{p_{\varnothing \to A}}{p_{A \to \varnothing}} = 0.00000614$
   - $S_A^{(2)} = 20$ means $\frac{p_{\varnothing \to A}}{p_{A \to \varnothing}} = 0.00000000206$
   - $\frac{p_{\varnothing \to A}}{p_{A \to \varnothing}}$ too small, will have big errorbars
   - For $S_A^{(2)} = 20$, one measurement requires as least 10^9 MC steps.
2. Ratio trick: $\frac{Z_{A_N}}{Z_{A_0}} = \frac{Z_{A_N}}{Z_{A_{N-1}}} \cdots \frac{Z_{A_{i+1}}}{Z_{A_i}} \cdots \frac{Z_{A_1}}{Z_{A_0}}$ **decompose!**
   - $\frac{Z_{A_{i+1}}}{Z_{A_i}}$ is easier to calculate
   - choosing A_{i+1} and A_i maybe tricky, some $\frac{Z_{A_{i+1}}}{Z_{A_i}}$ are small, some maybe quite large
   - requires many CPUs (proportional to L)
   - doesn't essentially improve computing efficiency

high precision!!

3.2 Nonequilibrium method

3.2.1 Jarzynski equality

F=ln(Z)
W>=Ff-Fi

The Jarzynski equality[5] states that

$$\left\langle \exp\left[-\beta \int_{t_i}^{t_f} dt \delta W(t)\right]\right\rangle = \frac{\mathcal{Z}_f}{\mathcal{Z}_i}$$

where $\delta W(t) = H(t+dt) - H(t)$ is the infinitesimal work.

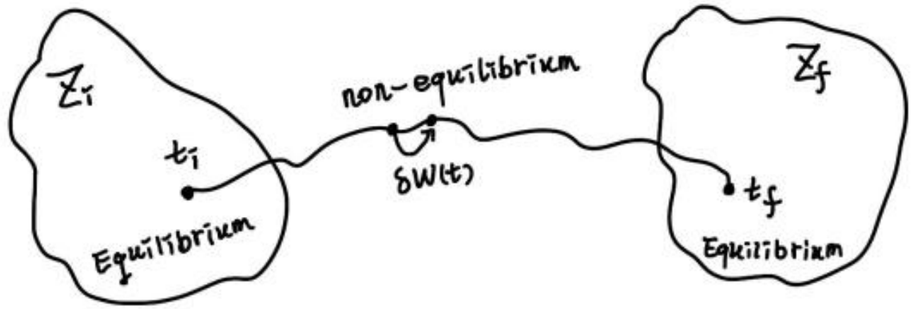

Recall that: $S_A^{(n)} = -\ln \frac{[\mathrm{Tr}_A(\rho_A^n)]}{1-n} = -\frac{1}{1-n} \ln\left[\frac{Z_A^{(n)}}{Z^{(n)}}\right]$

So that $S_A^{(n)} = \frac{1}{1-n} \ln\left\langle \exp(-\beta \int_{t_i}^{t_f} dt \delta W(t))\right\rangle$ [6]

[5] Jarzynski, C. *Phys. Rev. Lett. 78, 2690 (1997).*
[6] *Alba, V. Phys. Rev. E, 95, 062132 (2017).*

3.2.2 Nonequilibrium method

Define: $Z_A^{(n)}(\lambda) = \sum_{B\subseteq A} \lambda^{N_B}(1-\lambda)^{N_A-N_B} Z_B^{(n)} = \sum_{B\subseteq A} g_A(\lambda, N_B)\, Z_B^{(n)} = \sum_{B\subseteq A} e^{-\beta[-\frac{1}{\beta}(\ln g_A(\lambda,N_B)+\ln Z_B^{(n)})]}$

Then $S_A^{(n)} = -\frac{1}{n-1}\ln\left[\frac{Z_A^{(n)}}{Z^{(n)}}\right] = -\frac{1}{n-1}\ln\left[\frac{Z_A^{(n)}(1)}{Z_A^{(n)}(0)}\right] = \frac{1}{(1-n)}\int_0^1 d\lambda \frac{\partial \ln Z_A^{(n)}(\lambda)}{\partial\lambda} = \boldsymbol{\frac{1}{1-n}\int_0^1 d\lambda \frac{\partial Z_A^{(n)}(\lambda)/\partial\lambda}{Z_A^{(n)}(\lambda)}}$

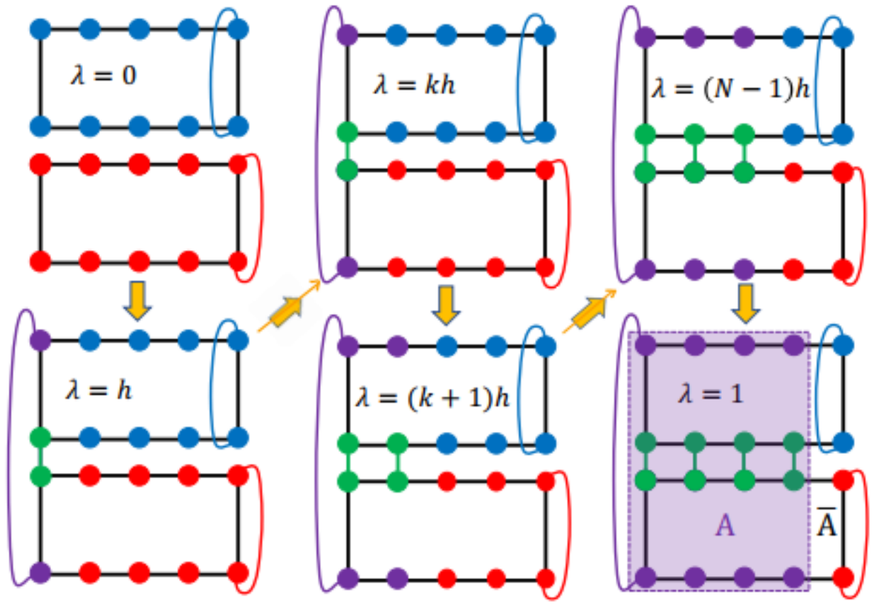

$$\langle \frac{N_B}{\lambda} - \frac{N_A - N_B}{1-\lambda} \rangle_\lambda$$

Probabilities[7]: $P_{\text{join}} = \min\left\{\frac{\lambda}{1-\lambda}, 1\right\} \quad P_{\text{leave}} = \min\left\{\frac{1-\lambda}{\lambda}, 1\right\}$

$$\delta W(t) = H(t+dt) - H(t) = -\frac{1}{\beta}[\ln g_A(\lambda(t+dt), N_B(t+dt)) - \ln g_A(\lambda(t), N_B(t))]$$

[7] D'Emidio, J. *Phys. Rev. Lett. 124*, 110602 (2020).
Alba, V. Phys. Rev. E, 95, 062132 (2017).

Better solution?

$$\frac{Z(\mathbf{p}')}{Z(\mathbf{p}'')} = \left\langle \frac{W(\mathbf{p}')}{W(\mathbf{p}'')} \right\rangle_{\mathbf{p}''}$$

$$\frac{Z(\mathbf{p}_0)}{Z(\mathbf{p}'')} = \prod_{k=1}^{m} \frac{Z(\mathbf{p}_{k-1})}{Z(\mathbf{p}_k)}$$

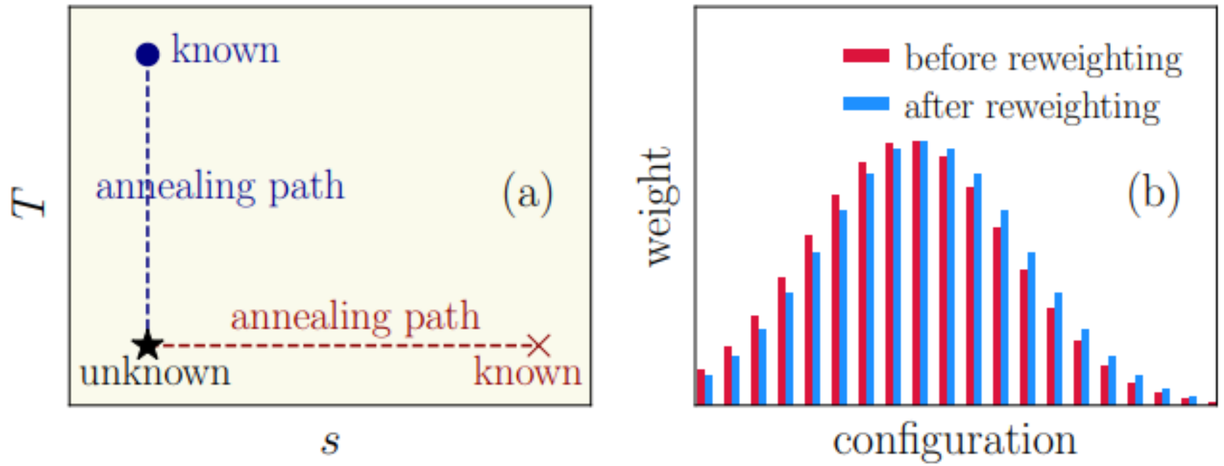

FIG. 1. Schematic diagram of the reweight-annealing method. (a) Finding a reference point and the annealing path connecting the unknown point to it in the parameter space. T and s correspond to the thermal and quantum version, respectively; (b) Using a sampled distribution (red) to represent another distribution (blue) through reweighting a same configuration. If these two distributions are close to each other, the effect of the reweighting would be good since the importance sampling can approximately be kept.

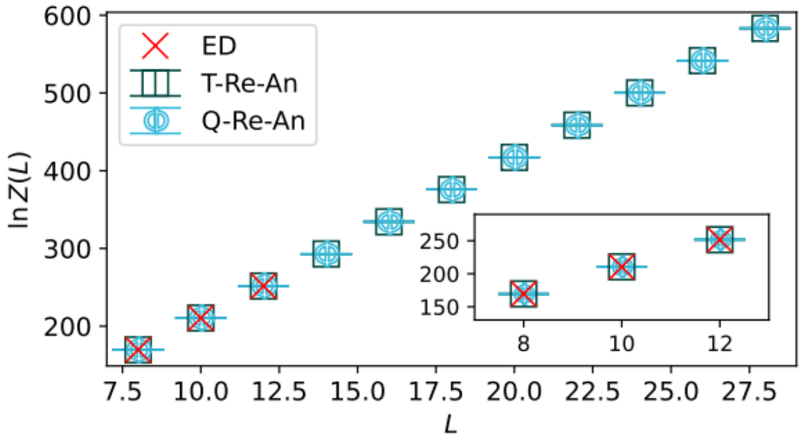

FIG. 2. For $\beta = 30$, the values of $\ln Z$ as a function of the chain length L, where both T-Re-An method and Q-Re-An method have a perfect match with ED. For example, for $L = 12$, the results from the two methods are 251.625(2) and 251.624(2), respectively, and the exact result is 251.62283 from ED calculations. Attention that here in practical SSE simulations, the Hamiltonian has a energy shift of $-1/4$ for each two-body term.

arXiv:2403.08642, Yi-Ming Ding, Jun-Song Sun, Nvsen Ma, Gaopei Pan, Chen Cheng, Zheng Yan

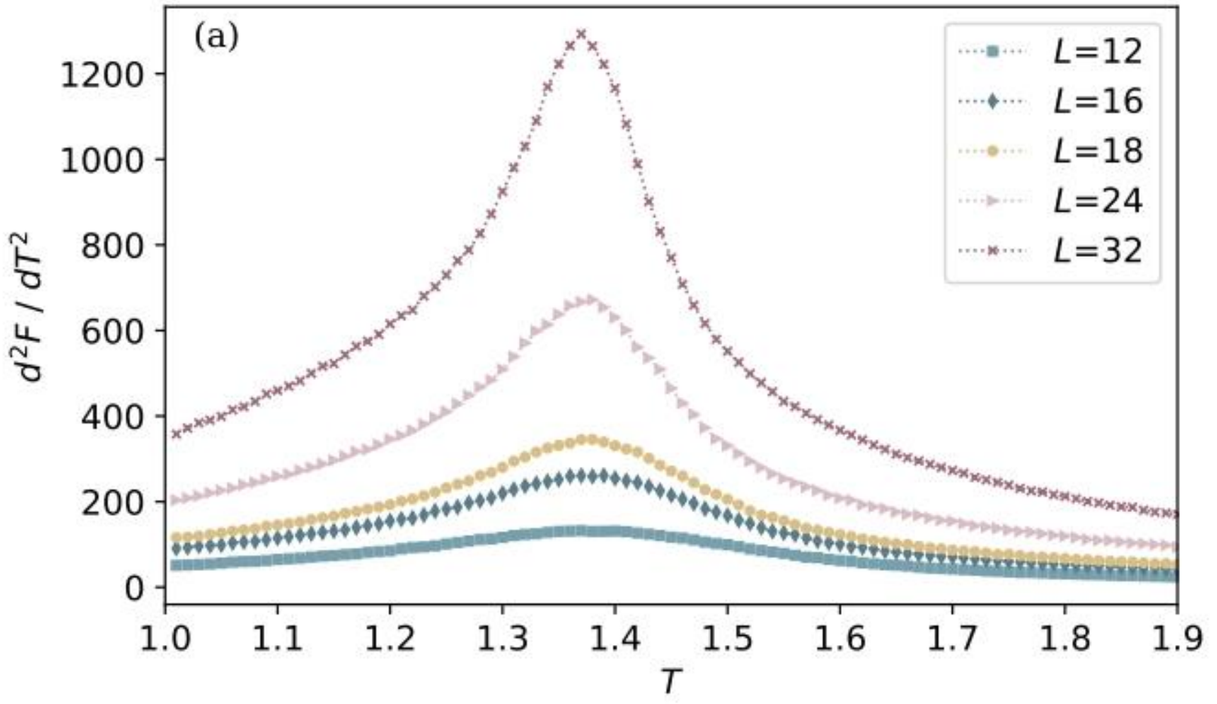

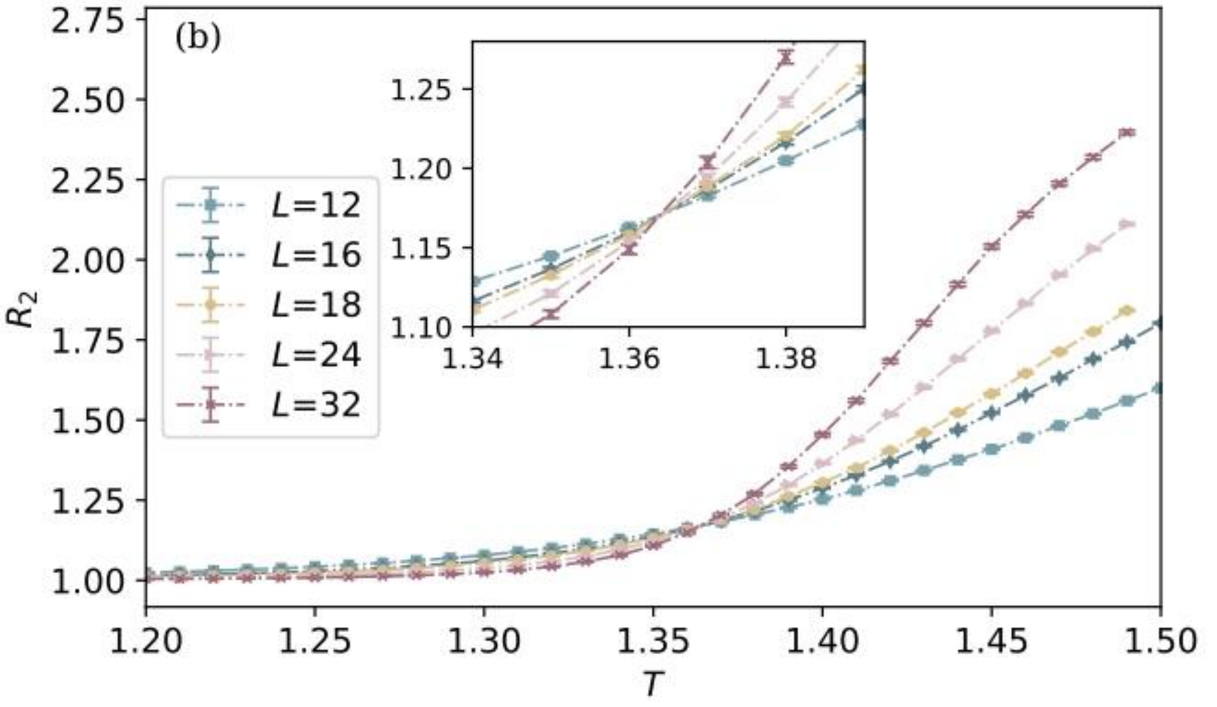

$$H = -\sum_{\langle i,j \rangle} [2S_i^z S_j^z + S_i^x S_j^x + S_i^y S_j^y]$$

$$-0.2 \sum_{\langle\langle i,j \rangle\rangle} [2S_i^z S_j^z + S_i^x S_j^x + S_i^y S_j^y].$$

FIG. 4. (a) The second order derivative of the free energy, $\partial^2 F/\partial T^2$, changes with the temperature T in different system size. The peak diverges more when the size becomes larger, which probes the phase transition point here; (b) The Binder ratios in this model at different sizes intersecting at a point which is highly consistent with the peak obtained by Re-An algorithm.

Probably the simplest and cheapest quantum Monte Carlo method so far for extracting high-precision entanglement entropy and its derivative

Zhe Wang,[1,2] Zhiyan Wang,[1,2] Yi-Ming Ding,[1,2] Bin-Bin Mao,[3] and Zheng Yan[1,2,*]

[1] *Department of Physics, School of Science and Research Center for Industries of the Future, Westlake University, Hangzhou 310030, China*

[2] *Institute of Natural Sciences, Westlake Institute for Advanced Study, Hangzhou 310024, China*

[3] *School of Foundational Education, University of Health and Rehabilitation Sciences, Qingdao 266000, China*

(Dated: June 11, 2024)

Measuring entanglement entropy (EE) to probe the intrinsic physics of quantum many-body systems is an important but challenging topic in condensed matter, high energy and computational physics. Designing quantum Monte Carlo (QMC) algorithm to obtain the Rényi EE is a promising solution in large-scale many-body systems. However, to gain high-precision EE, the QMC-based algorithm for EE becomes more and more complex at the designing level. The entangled region needs being changed during the QMC simulation, and the detailed balance condition becomes more complicated. Moreover, the intermediately incremental processes introduced cannot be exploited neither. In this paper, we propose a simple QMC scheme able to extract EE and its derivative with high-precision, which requires neither changing replica manifold during the simulation nor adding extra detailed balance conditions. All the values measured in the incremental process are the EE under physical parameters, which greatly improves the efficiency. It opens an access to numerically probe the novel phases and phase transitions by scanning EE in a wide parameter-region in 2D and higher dimensional systems. The method has low-technical barrier and is natural for parallel computing. Our algorithm makes it no longer a dream to calculate a large amount of high-precision EE values without complicated techniques and huge computational cost.

arXiv:2406.05324 (2024)

$$Z_A^{(n)}(J')/Z^n(J') \;=?$$

- $Z_A^{(n)}(J')/Z_A^{(n)}(J)$
- $Z(J')/Z(J)$
- $Z_A^{(n)}(J)/Z^n(J)$

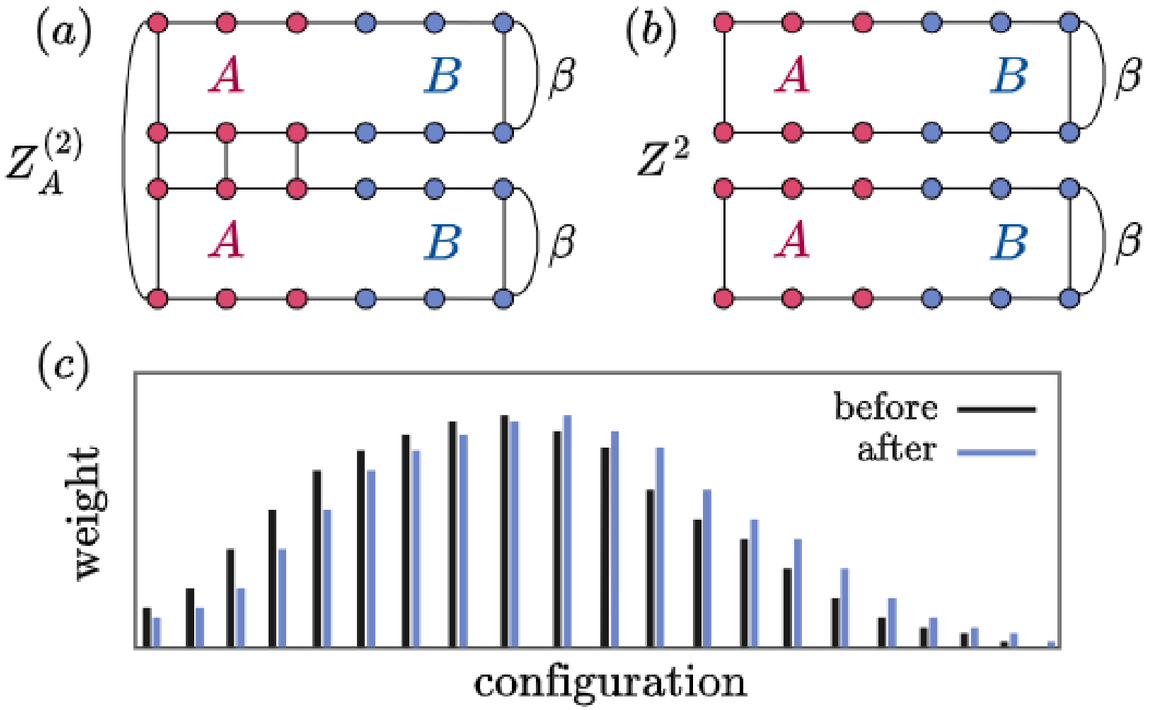

$$\frac{Z_A^{(n)}(J')}{Z_A^{(n)}(J)} = \left\langle \frac{W(J')}{W(J)} \right\rangle_{Z_A^{(n)}(J)}$$

$$\frac{Z_A^{(n)}(J')}{Z_A^{(n)}(J)} = \prod_{i=0}^{N-1} \frac{Z_A^{(n)}(J_{i+1})}{Z_A^{(n)}(J_i)}$$

$$H = J_1 \sum_{\langle ij \rangle} S_i S_j + J_2 \sum_{\langle ij \rangle} S_i S_j$$

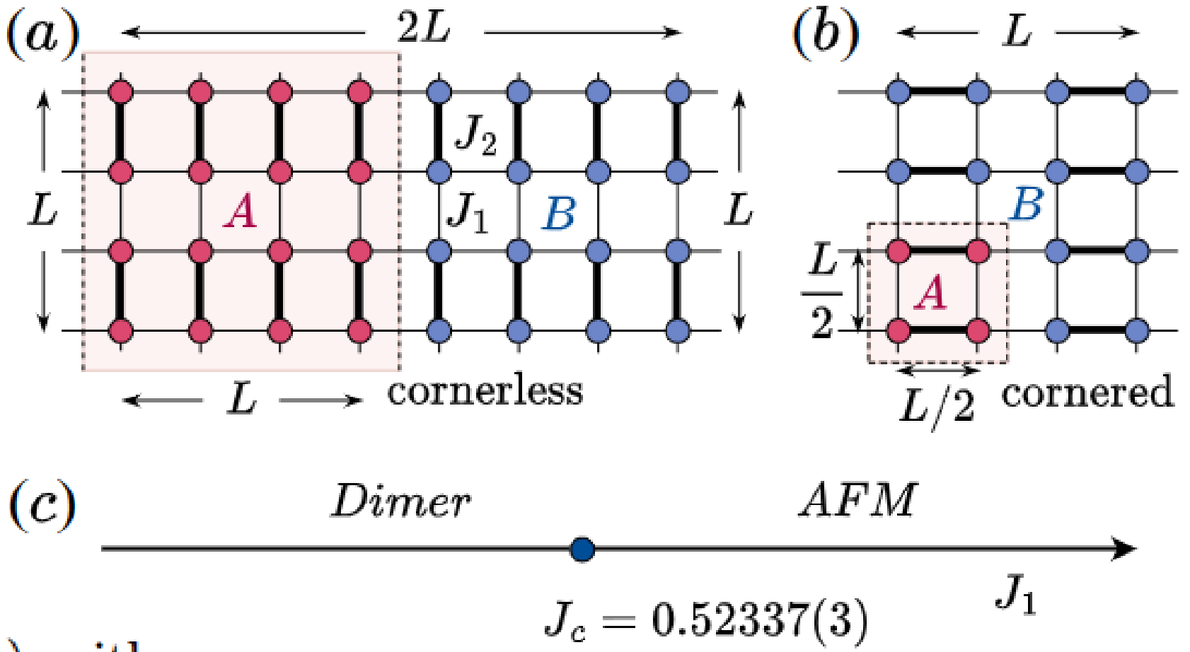

TABLE I. Fitting results for the data in Fig.3 (a_1) with $S^{(2)}(l) = al + b\ln l - c$. Reduced and p-value of χ^2 (R/P-χ^2) are also listed.

J_1	a	b	c	R/P-χ^2
1.0	0.089(2)	1.05(4)	1.61(9)	1.00/0.40
0.9	0.085(2)	1.02(3)	1.54(7)	0.54/0.71
0.8	0.079(2)	1.06(5)	1.6(1)	1.55/0.19
0.6	0.072(2)	1.06(5)	2.0(2)	1.93/0.10
0.55	0.078(3)	0.8(1)	1.6(2)	3.16/0.02
0.54	0.08(1)	0.6(1)	1.2(2)	2.49/0.04
$J_c = 0.52337$	0.8(1)	0.15(17)	0.1(5)	2.02/0.1

$$\frac{Z_A^{(n)}(J_1')}{Z_A^{(n)}(J_1)} = \left\langle \left(\frac{J_1'}{J_1}\right)^{n_{J_1}} \right\rangle_{Z_A^{(n)}(J_1)}$$

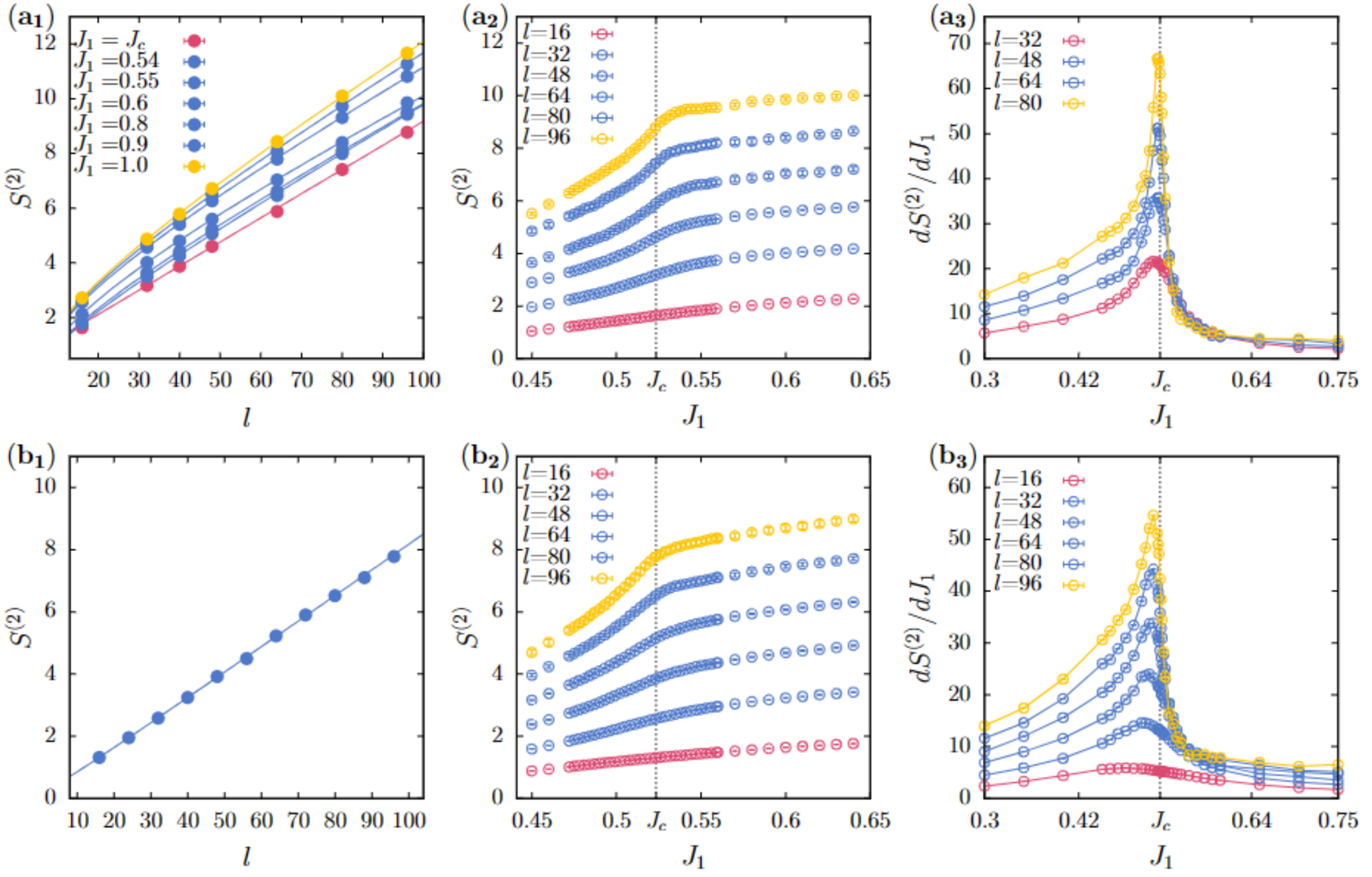

FIG. 3. Second Rényi entanglement entropy $S^{(2)}$ of the $J_1 - J_2$ Heisenberg model with the entanglement region A cornerless [(a_1),(a_2) and (a_3)] or cornered [(b_1),(b_2) and (b_3)]. Cornerless see Fig.2 (a) and cornered see Fig.2 (b). (a_1) $S^{(2)}$ versus l for different couplings J_1. The fitting results are listed in Table I. (b_1) $S^{(2)}$ versus l at the QCP $J_1 = J_c = 0.52337$. The fitting result is $S^{(2)}(l) = 0.083(1)l - 0.08(1)\ln l + 0.19(2)$ with R/P-χ^2 are 0.85/0.56. [(a_2) and (b_2)] $S^{(2)}$ versus couplings J_1 for different l to identify the critical point. [(a_3) and (b_3)] The derivative of $S^{(2)}$, $dS^{(2)}/dJ_1$, versus couplings J_1 for different l. The peaks of $dS^{(2)}/dJ_1$ appear at the QCP J_c.

EE derivative.- It can be proved in the SI that the derivative of the nth Rényi EE can be measured in the form:

$$\frac{dS^{(n)}}{dJ} = \frac{1}{1-n}\left[-n\beta\left\langle \frac{dH}{dJ} \right\rangle_{Z_A^{(n)}} + n\beta\left\langle \frac{dH}{dJ} \right\rangle_{Z}\right] \quad (5)$$

where the J is a general parameter and n is the Rényi index, the first average is based on the distribution of $Z_A^{(n)}$ and the second is Z. Taking the $J_1 - J_2$ model as an example with fixed $J_2 = 1$ and $n = 2$, set J_1 as the tunable parameter here and note H is a linear function of J_1, the Eq.(5) becomes $dS^{(2)}/dJ_1 = 2\beta\langle H_{J_1}/J_1\rangle_{Z_A^{(2)}} - 2\beta\langle H_{J_1}/J_1\rangle_Z$, where the H_{J_1} means the J_1 term of the H. In the SSE frame, it is similar as measuring energy value, which is very simple. The details can be found in the SI.

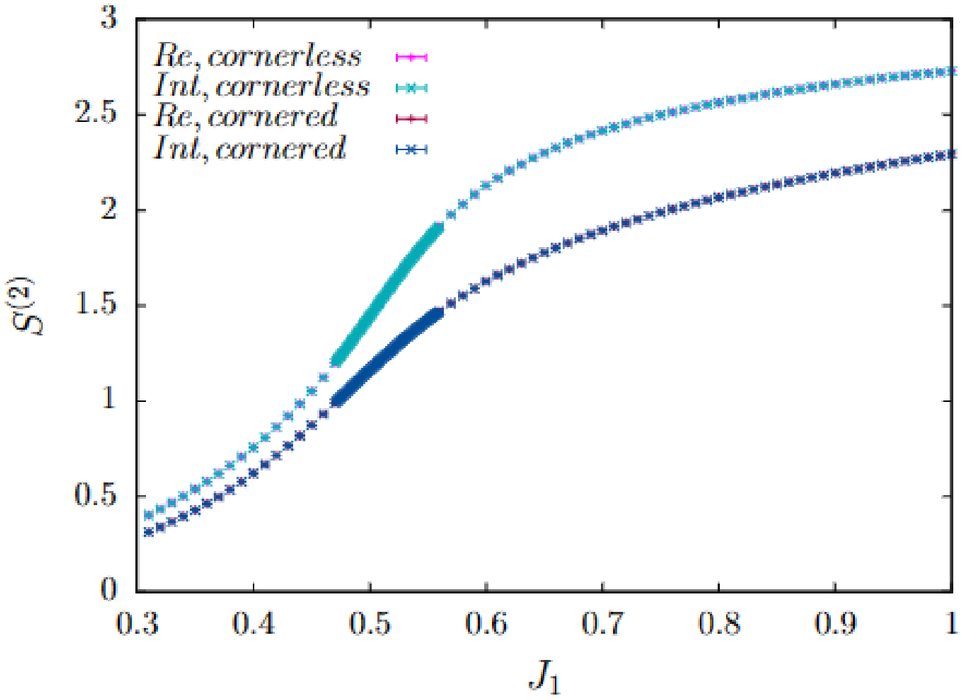

FIG. 4. Second Rényi entanglement entropy $S^{(2)}$ of the J_1-J_2 Heisenberg model as a function of the coupling J_1 are calculated by Reweight method (Re) and integral method (Int) either in cornerless or cornered entanglement region A with $l = 16$. With or without corners, the results are consistent within errorbar for two methods.

Entanglement Spectrum

- Break

Entanglement Spectrum as a Generalization of Entanglement Entropy: Identification of Topological Order in Non-Abelian Fractional Quantum Hall Effect States

Hui Li and F. D. M. Haldane

Physics Department, Princeton University, Princeton, New Jersey 08544, USA

(Received 2 May 2008; published 3 July 2008)

We study the ''entanglement spectrum'' (a presentation of the Schmidt decomposition analogous to a set of ''energy levels'') of a many-body state, and compare the Moore-Read model wave function for the $\nu = 5/2$ fractional quantum Hall state with a generic $5/2$ state obtained by finite-size diagonalization of the second-Landau-level-projected Coulomb interactions. Their spectra share a common ''gapless'' structure, related to conformal field theory. In the model state, these are the *only* levels, while in the ''generic'' case, they are separated from the rest of the spectrum by a clear ''entanglement gap'', which appears to remain finite in the thermodynamic limit. We propose that the low-lying entanglement spectrum can be used as a ''fingerprint'' to identify topological order.

$$\rho_A = e^{-\mathcal{H}_A}$$

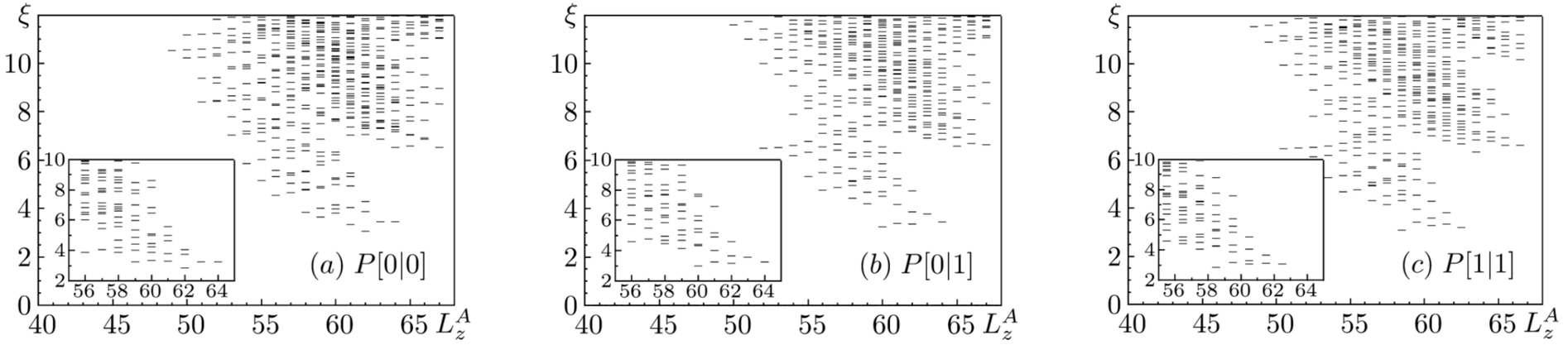

Entanglement Spectra of Quantum Heisenberg Ladders

Didier Poilblanc

Laboratoire de Physique Théorique UMR5152, CNRS and Université de Toulouse, F-31062 France

(Received 19 May 2010; revised manuscript received 29 June 2010; published 13 August 2010)

Bipartite entanglement measures are surprisingly useful tools to investigate quantum phases of correlated electrons. Here, I analyze the entanglement spectrum of *gapped* two-leg quantum Heisenberg ladders on a periodic ribbon partitioned into two identical periodic chains. The entanglement spectrum closely reflects the low-energy gapless spectrum of each individual edge. This extends the conjecture initially drawn for fractional quantum Hall systems to the field of quantum magnetism, stating a direct correspondence between the low-energy entanglement spectrum of a partitioned system and the true spectrum of the *virtual edges*. A mapping of the reduced density matrix to a thermodynamic density matrix is also proposed via the introduction of an effective temperature.

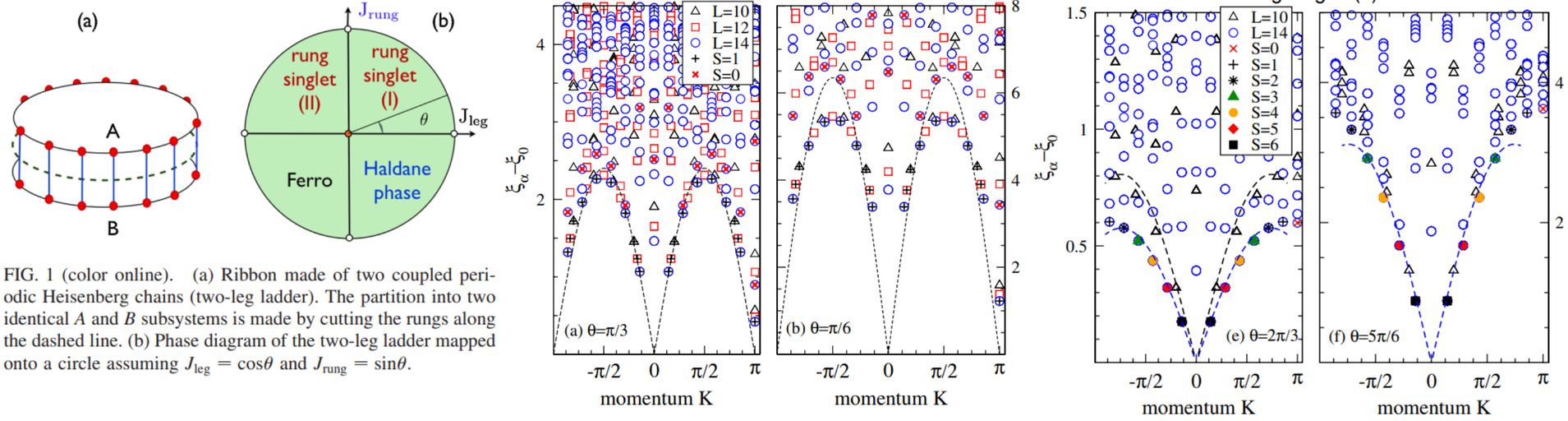

FIG. 1 (color online). (a) Ribbon made of two coupled periodic Heisenberg chains (two-leg ladder). The partition into two identical A and B subsystems is made by cutting the rungs along the dashed line. (b) Phase diagram of the two-leg ladder mapped onto a circle assuming $J_{leg} = \cos\theta$ and $J_{rung} = \sin\theta$.

General Relationship between the Entanglement Spectrum and the Edge State Spectrum of Topological Quantum States

Xiao-Liang Qi,[1,2] Hosho Katsura,[3,4] and Andreas W. W. Ludwig[5]

[1]*Department of Physics, Stanford University, Stanford, California 94305, USA*
[2]*Microsoft Research, Station Q, University of California, Santa Barbara, California 93106, USA*
[3]*Kavli Institute for Theoretical Physics, University of California, Santa Barbara, California 93106, USA*
[4]*Department of Physics, Gakushuin University, Mejiro, Toshima-ku, Tokyo 171-8588, Japan*
[5]*Department of Physics, University of California, Santa Barbara, California 93106, USA*

(Received 26 June 2011; published 10 May 2012)

We consider (2 + 1)-dimensional topological quantum states which possess edge states described by a chiral (1 + 1)-dimensional conformal field theory, such as, e.g., a general quantum Hall state. We demonstrate that for such states the reduced density matrix of a finite spatial region of the gapped topological state is a thermal density matrix of the chiral edge state conformal field theory which would appear at the spatial boundary of that region. We obtain this result by applying a physical instantaneous cut to the gapped system and by viewing the cutting process as a sudden "quantum quench" into a conformal field theory, using the tools of boundary conformal field theory. We thus provide a demonstration of the observation made by Li and Haldane about the relationship between the entanglement spectrum and the spectrum of a physical edge state.

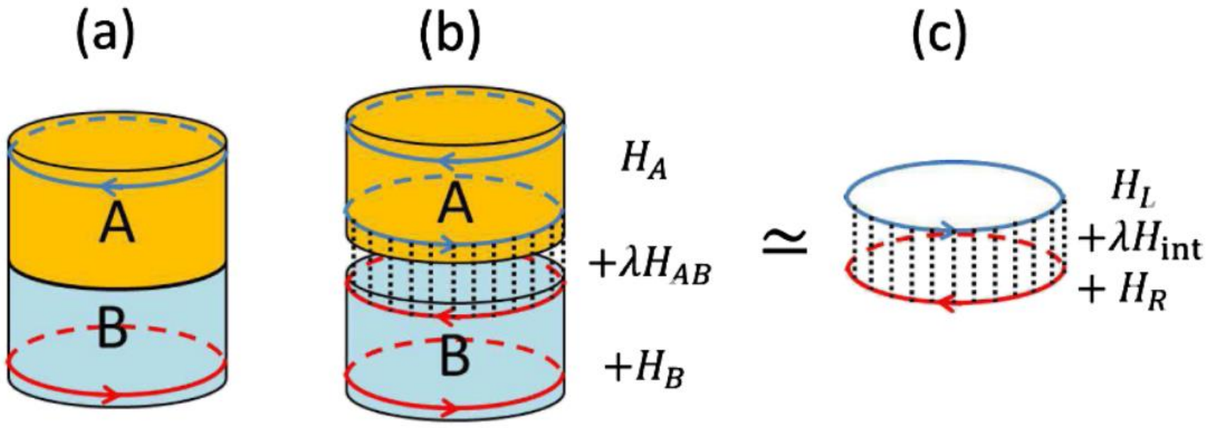

Quantum Monte Carlo??
Spectrum ????

$$S(\omega) = \frac{1}{\pi}\sum_{m,n} e^{-\beta E_n} |\langle m|\mathcal{O}|n\rangle|^2 \delta(\omega - [E_m - E_n]).$$

$$G(\tau) = \int_0^\infty d\omega K(\omega,\tau) S(\omega).$$

Stochastic **analytic continuation**!!

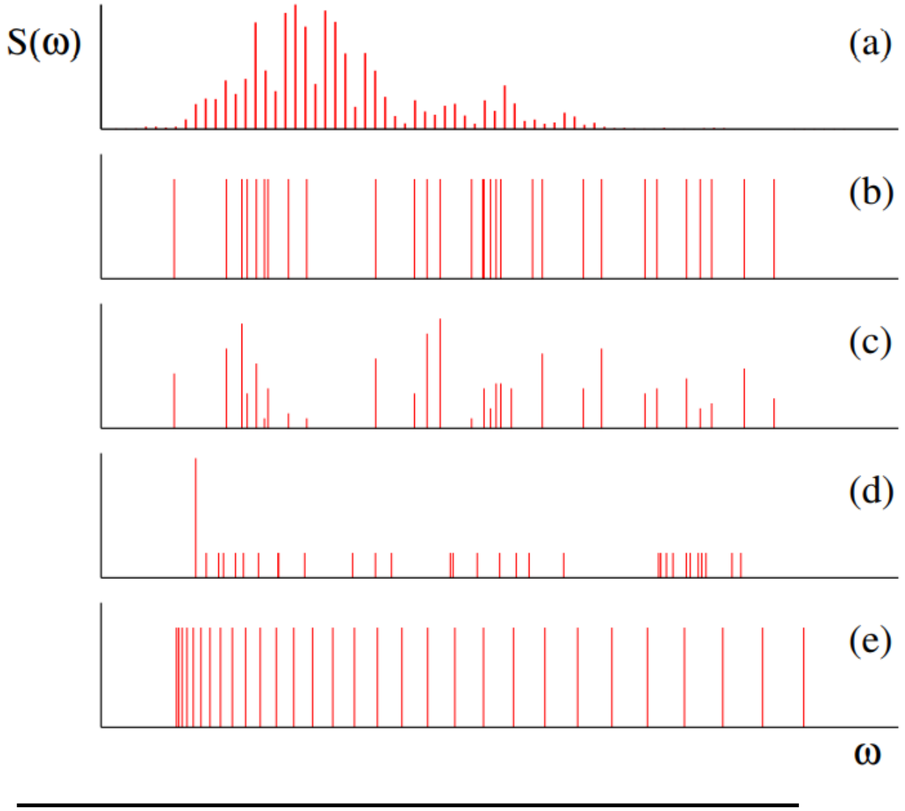

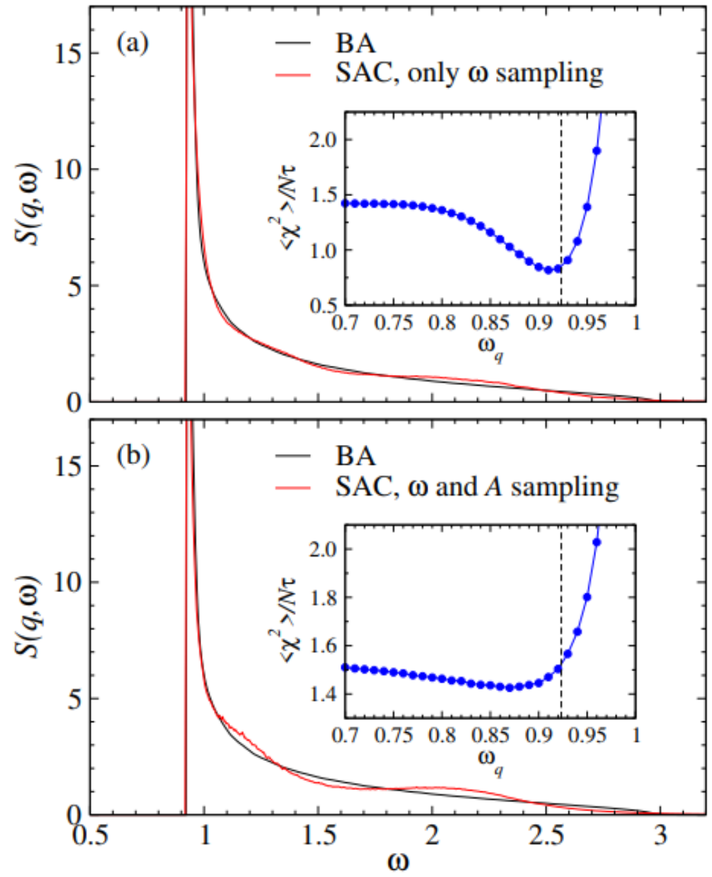

Sandvik, A., Phys. Rev. B **57** 10287 (1998); Sandvik, A., Phys. Rev. E **94**, 063308 (2016).

Syljuåsen, O., Phys. Rev. B **78**, 174429 (2008); Shao, H. and Sandvik, A., arXiv:2202.09870 (2022)

Quantum Monte Carlo simulation!!
Entanglement Spectrum !!!

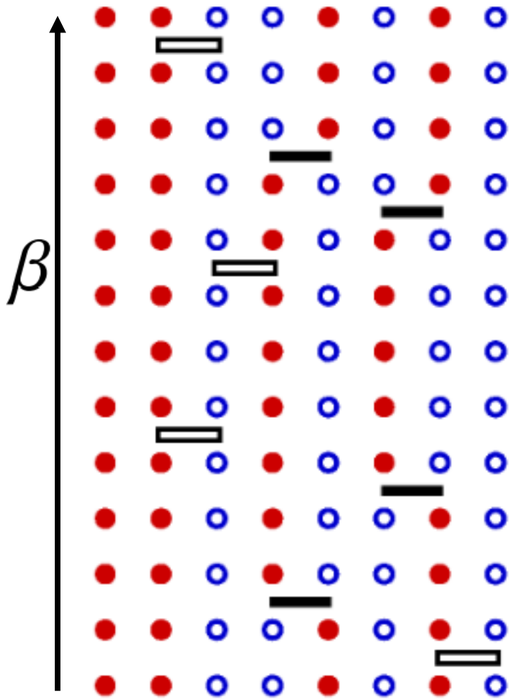

$$\rho_A = e^{-\mathcal{H}_A}$$

$$\mathcal{Z}_A^{(n)} = \mathrm{Tr}[\rho_A^n] = \mathrm{Tr}[e^{-n\mathcal{H}_A}].$$

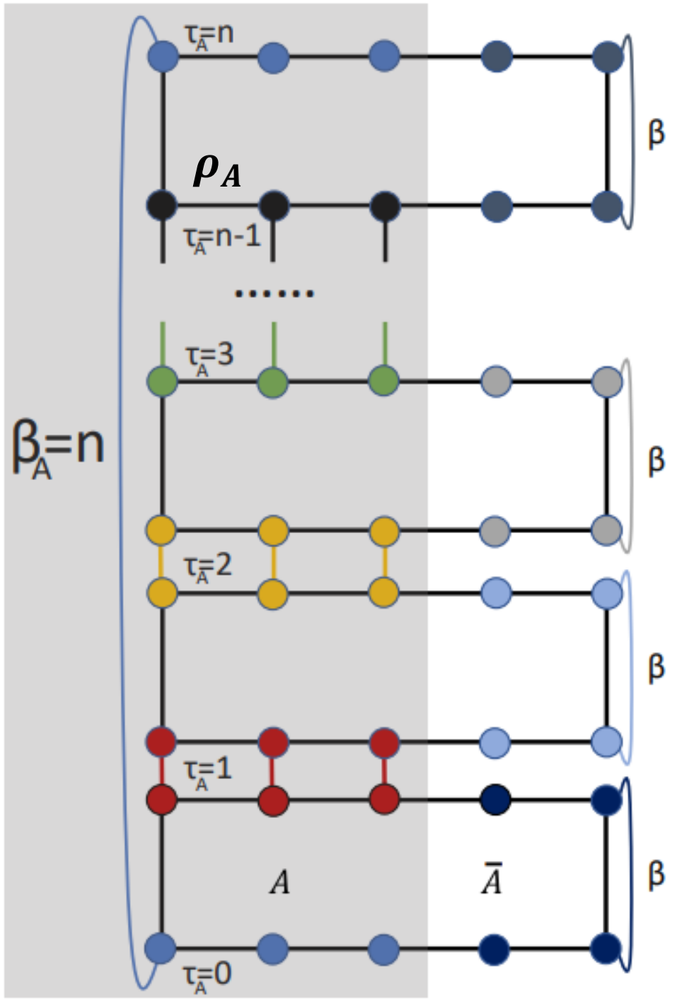

Zheng Yan*, Z. Y. Meng, *Nat. Commun. 14, 2360 (2023)*

Example 1: Ladder

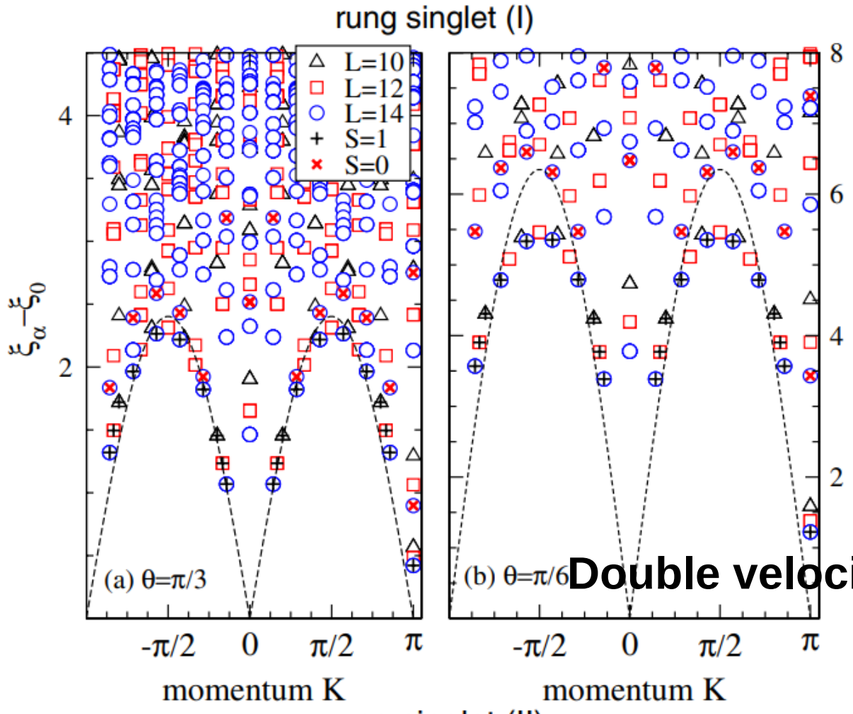

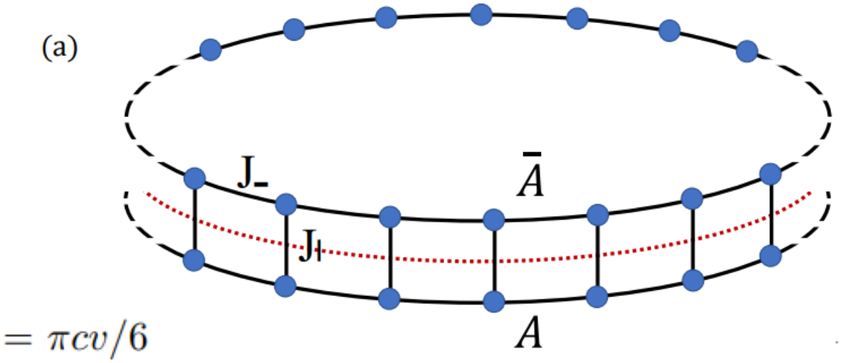

$$\xi_0/L = e_0 + d_1/L^2 + \mathcal{O}(1/L^3) \text{ where the } d_1 = \pi cv/6$$

Double velocity (slope) correction!

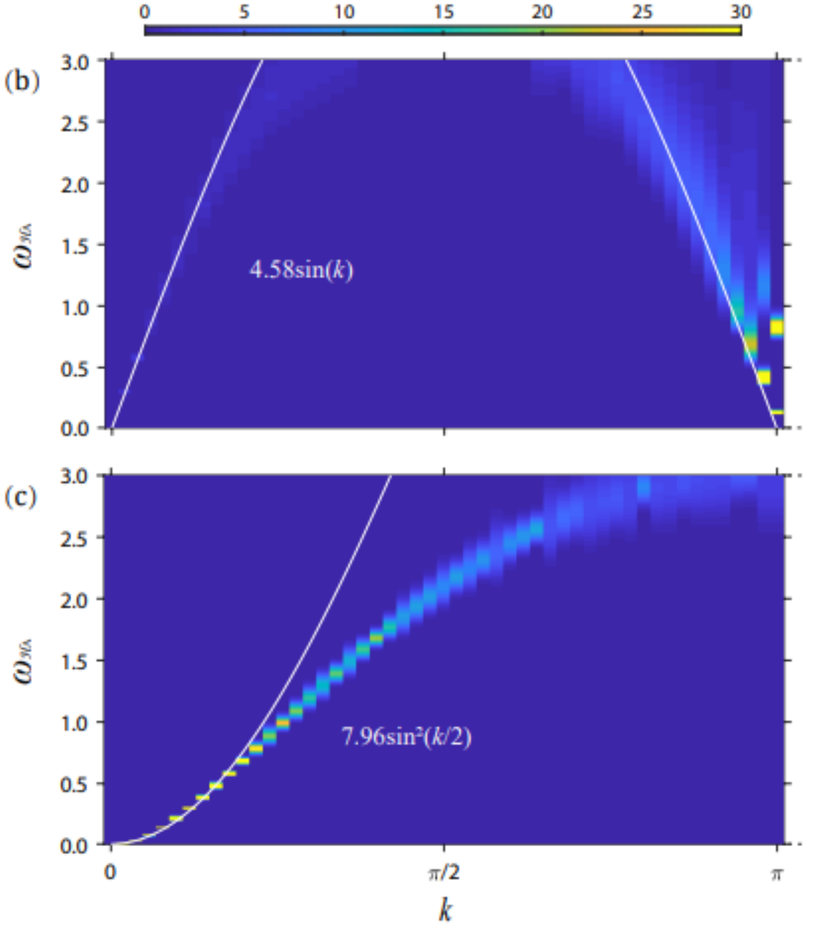

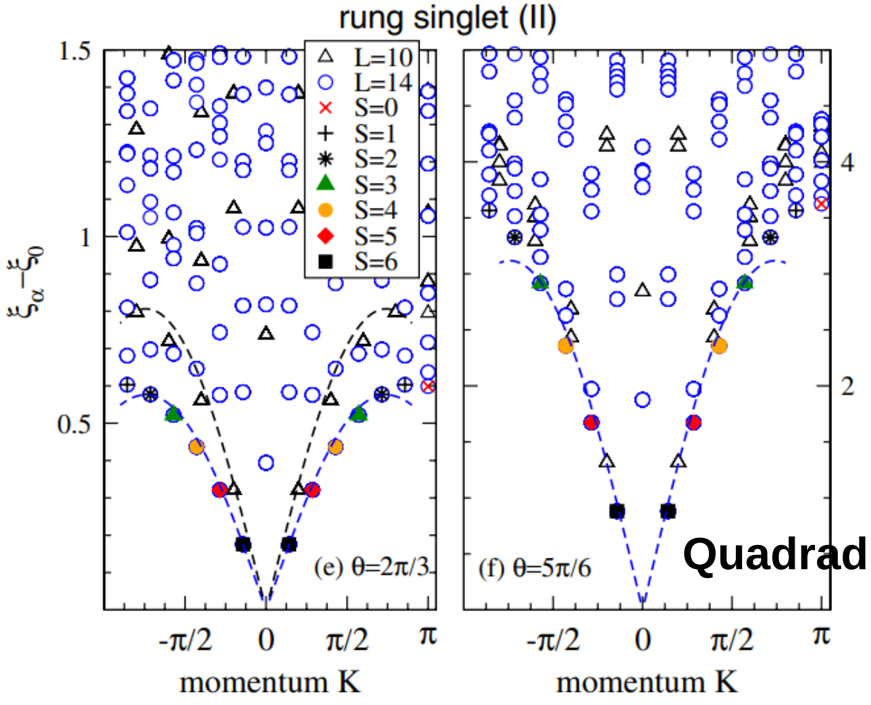

Quadradic dispersion!

Example 2: Bilayer

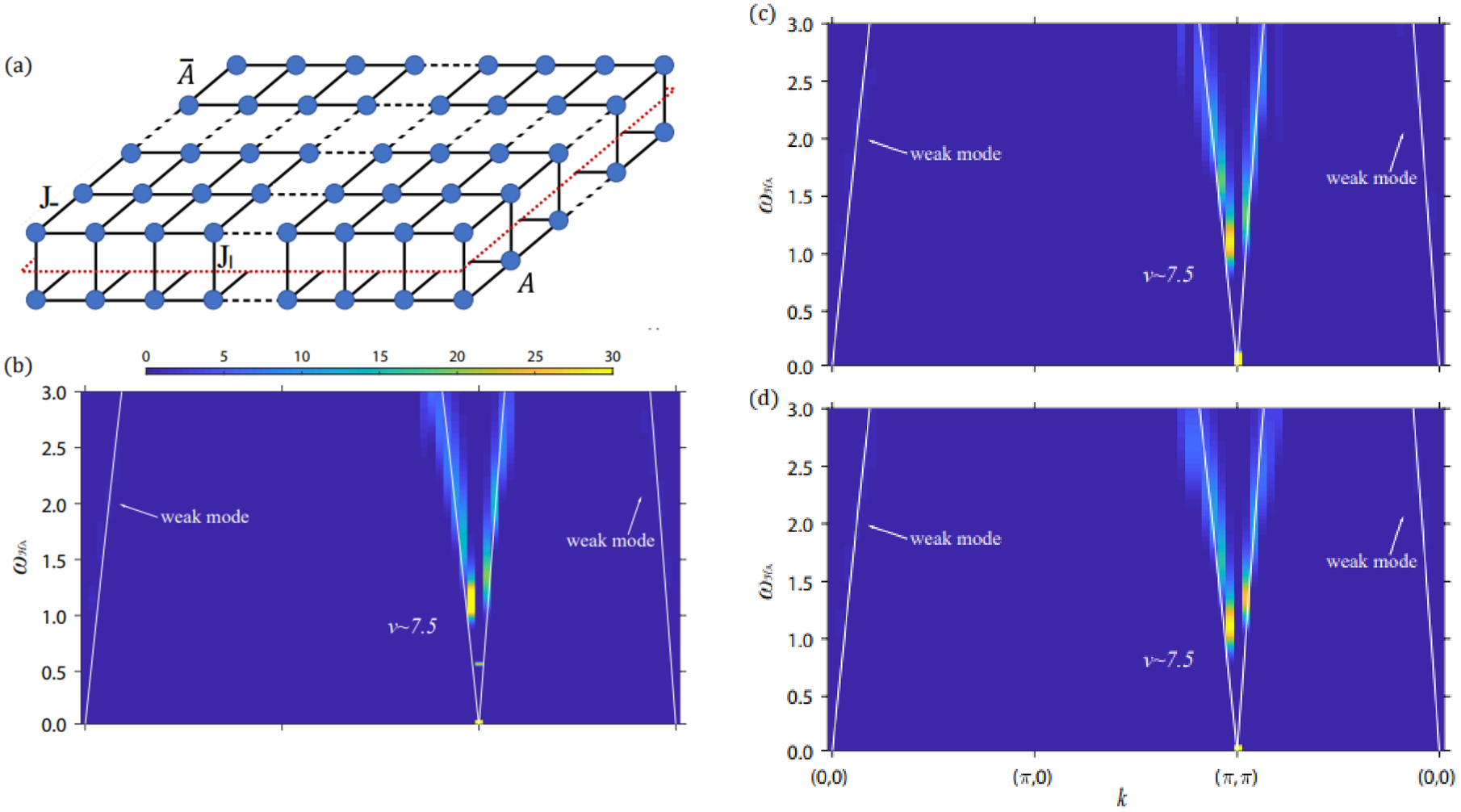

The results reveal that the deep correspondence between the ground state ES of a many-body system of entangled constituents with the true spectra on their virtual edges, is robust across (2+ 1)d quantum phase transitions

The wormhole effect on the path integral of reduced density matrix: Unlock the mystery of energy spectrum and entanglement spectrum

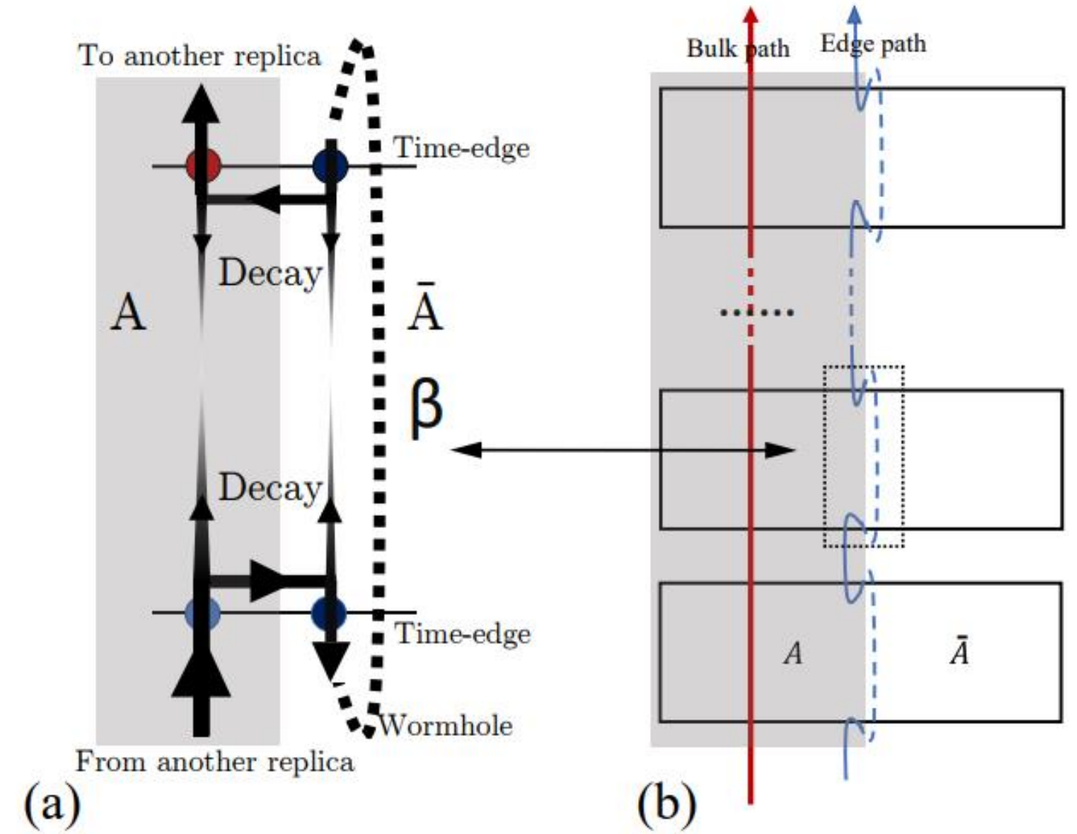

$$\beta\Delta_b : \Delta_e$$

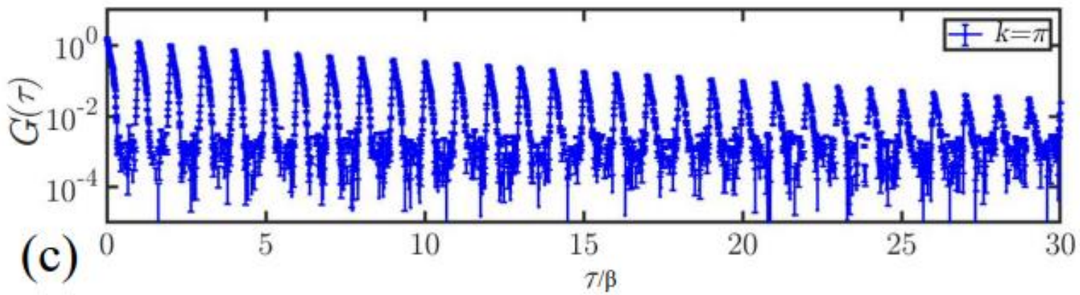

Extending Li-Haldane conjecture: Engineering the entanglement spectrum

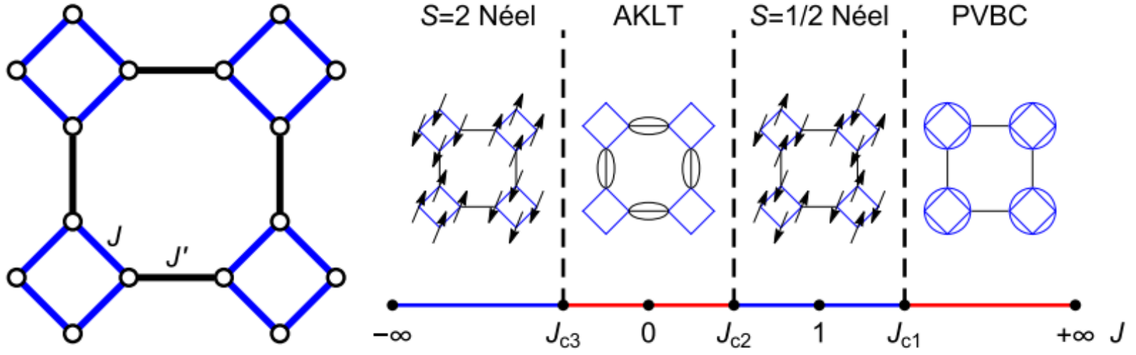

Z. Liu, **Zheng Yan*,** et al. Phys. Rev. B, 105, 014418 (2022).

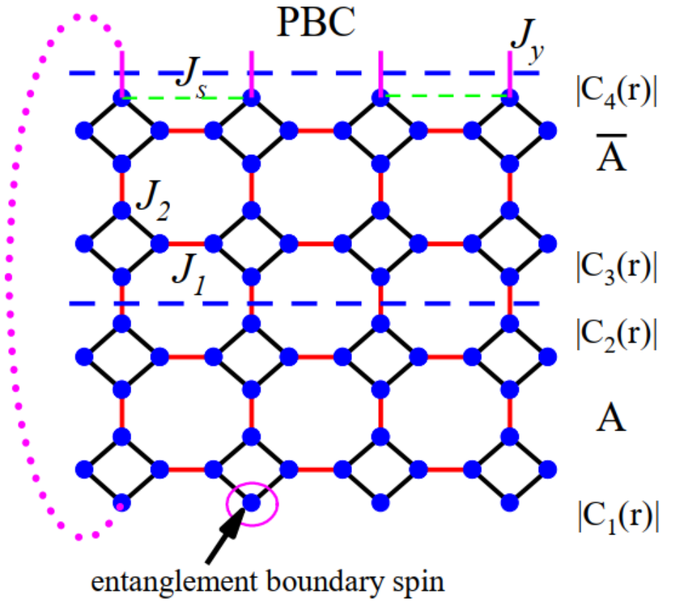

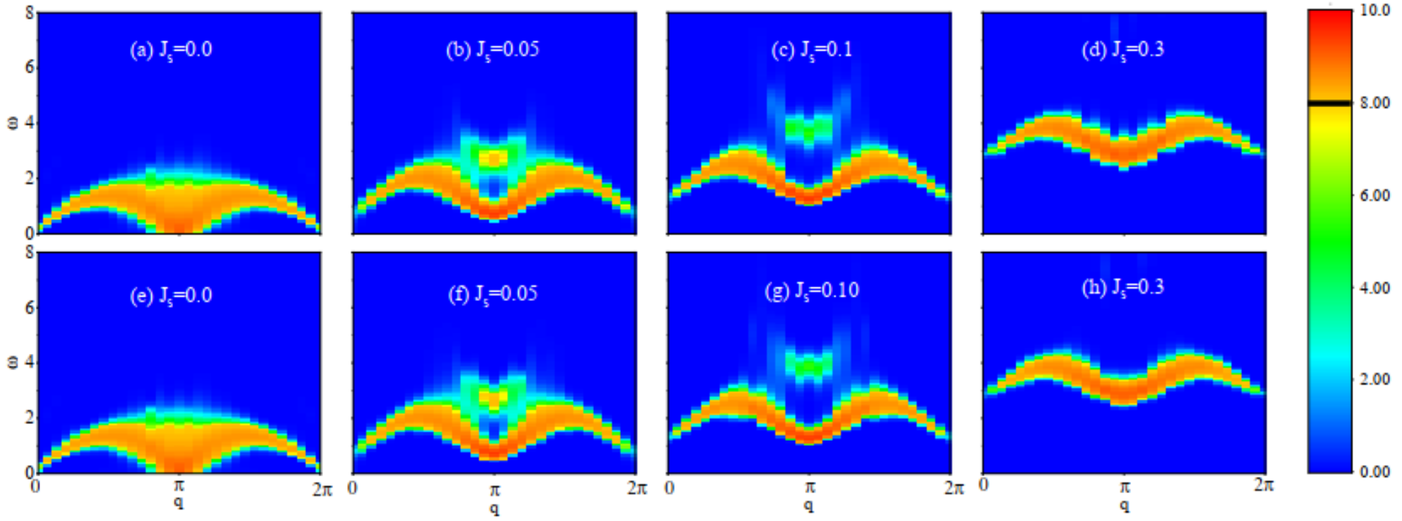

Z. Liu, **Zheng Yan*,** et al, Phys. Rev. B 109, 094416 (2024)

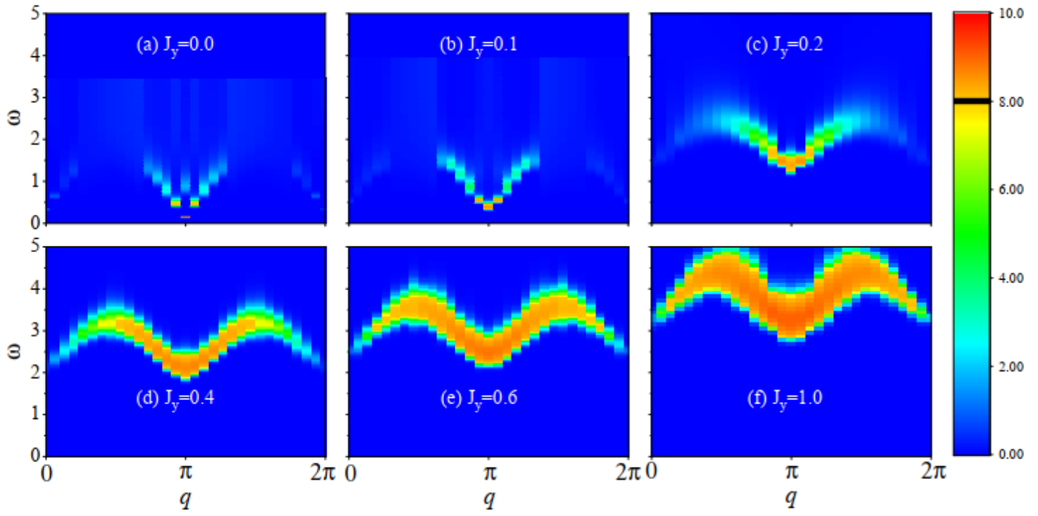

$$\beta\Delta_b \ : \ \Delta_e$$

Reversing the Li and Haldane conjecture: The low-lying entanglement spectrum resembles the bulk energy spectrum

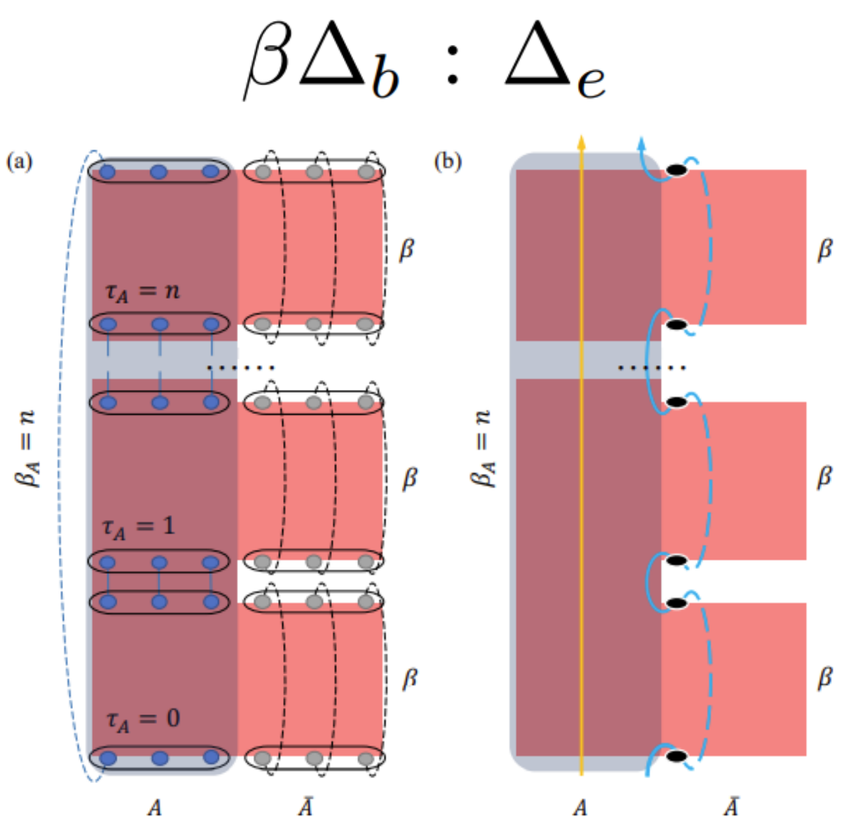

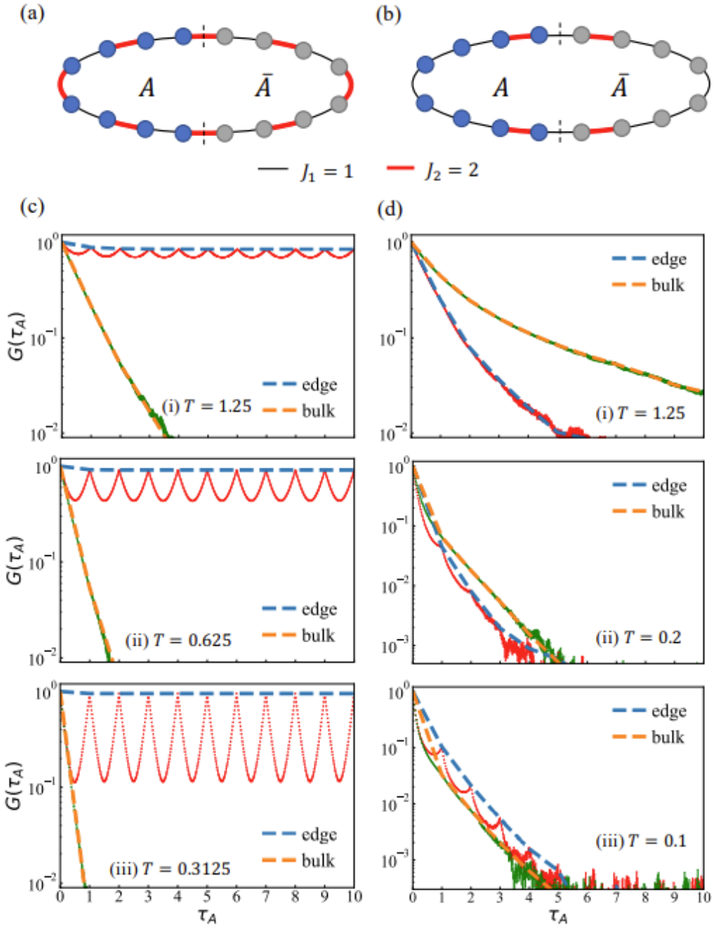

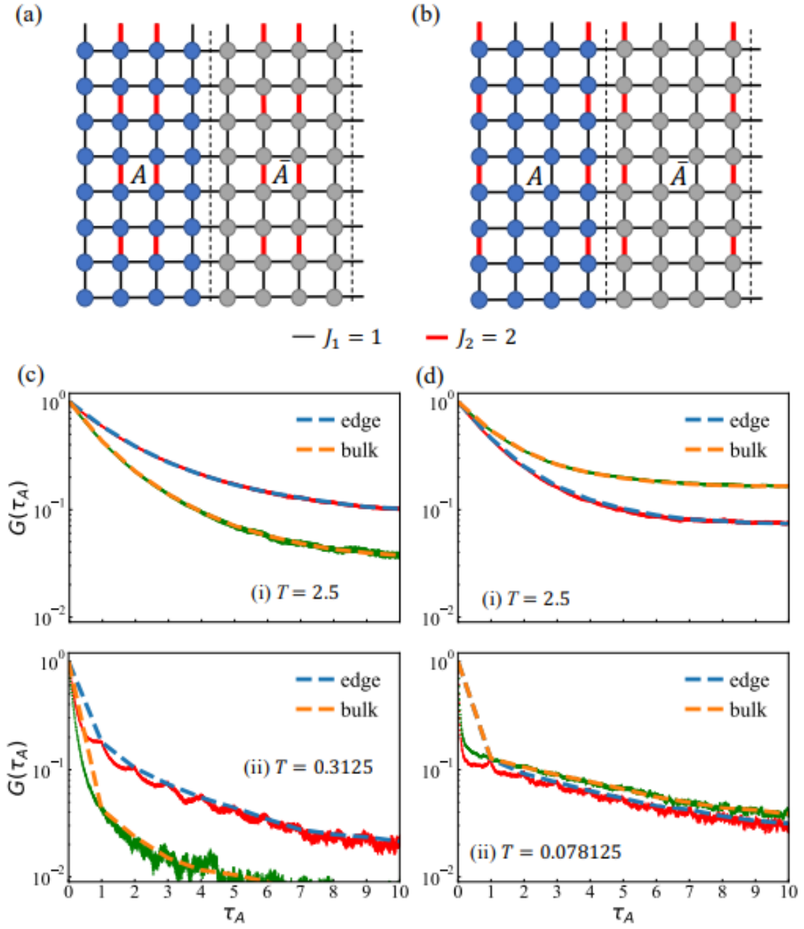

M. Song, **Zheng Yan***, et al. Phys. Rev. B 108, 075114 (2023)

$$\rho_A^n = e^{-n\mathcal{H}_A}$$

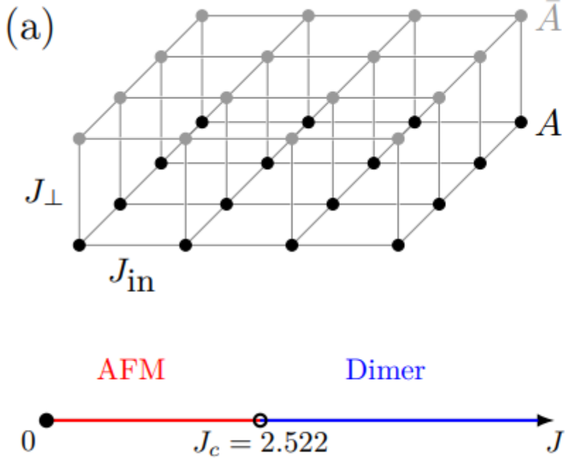

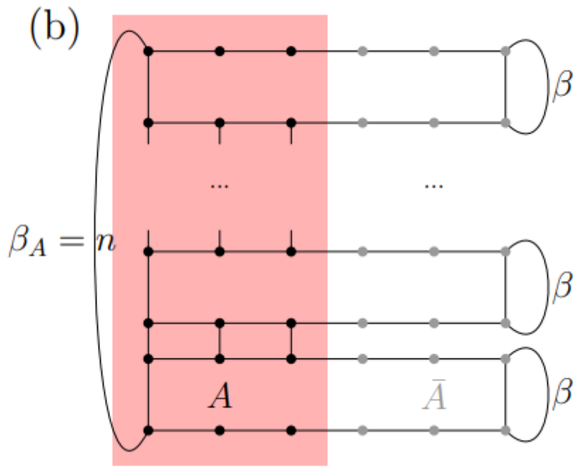

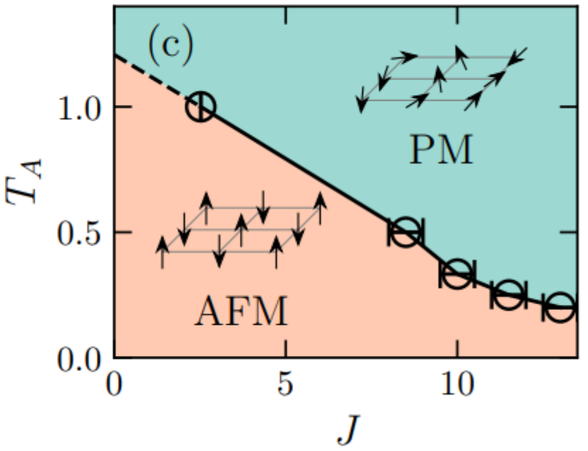

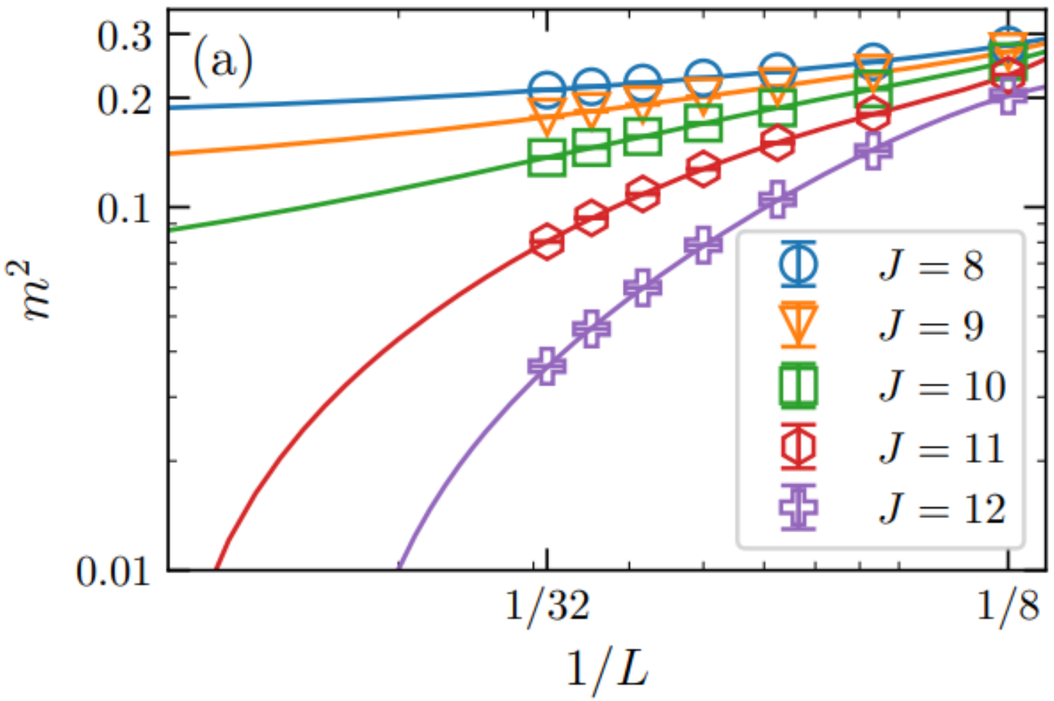

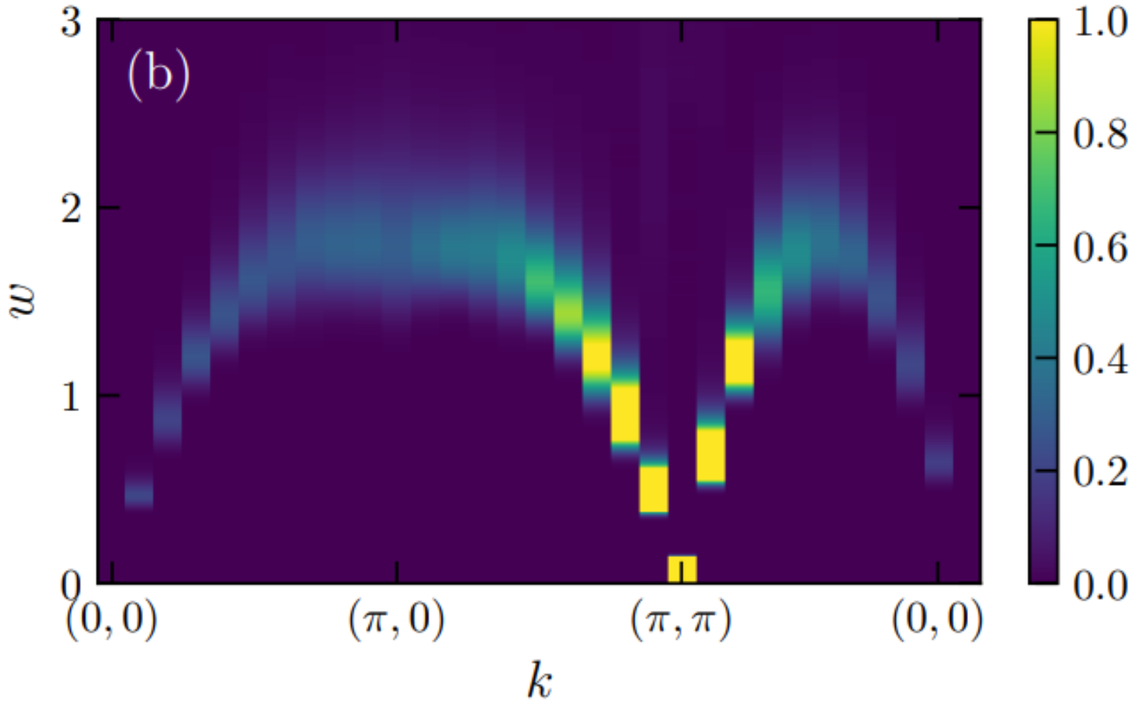

Chuhao Li, **Zheng Yan***, et al, arXiv: 2309. 16089 (2023)

Sampling reduced density matrix to extract fine levels of entanglement spectrum

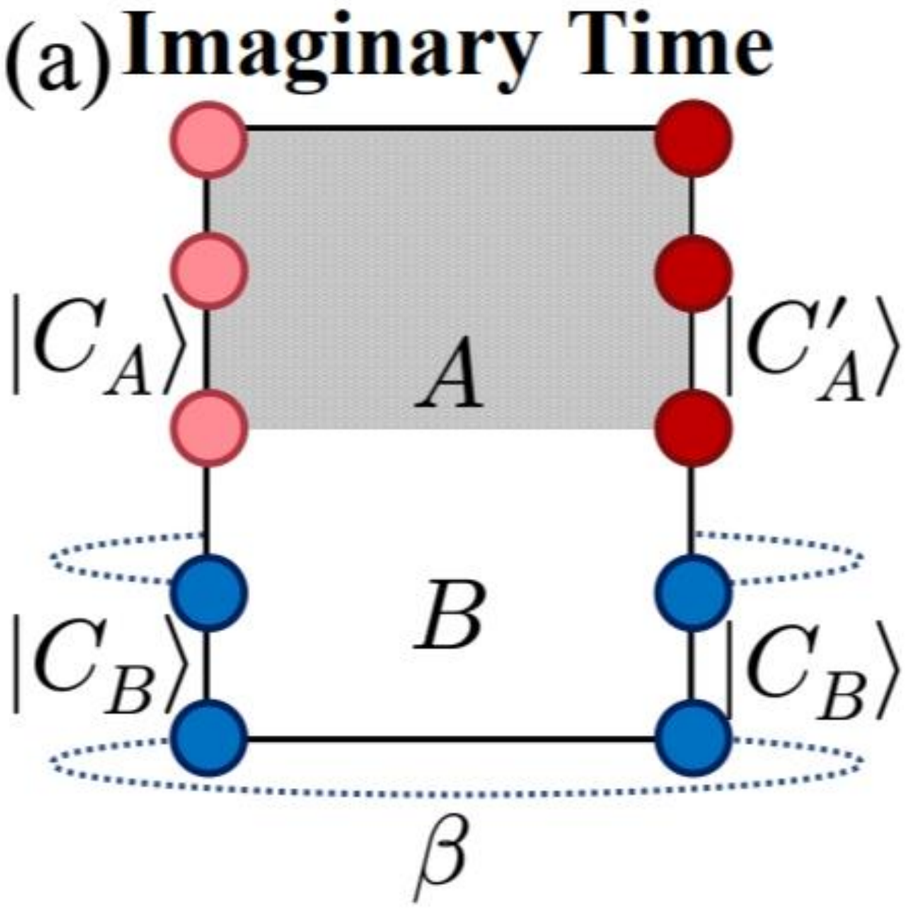

$$\rho_A = \mathrm{Tr}_B(\rho)$$

Bin-Bin Mao, Yi-Ming Ding, Zheng Yan
arXiv: 2310. 16709 [quant-ph] (2023)

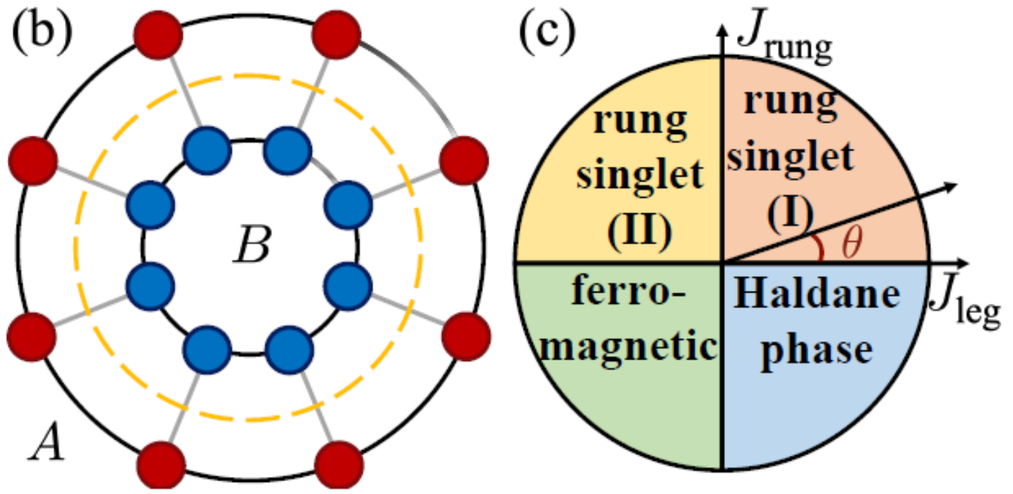
(b)
B
A

(c)
$J_{\rm rung}$
rung singlet (II)
rung singlet (I)
θ
ferro-magnetic
Haldane phase
$J_{\rm leg}$

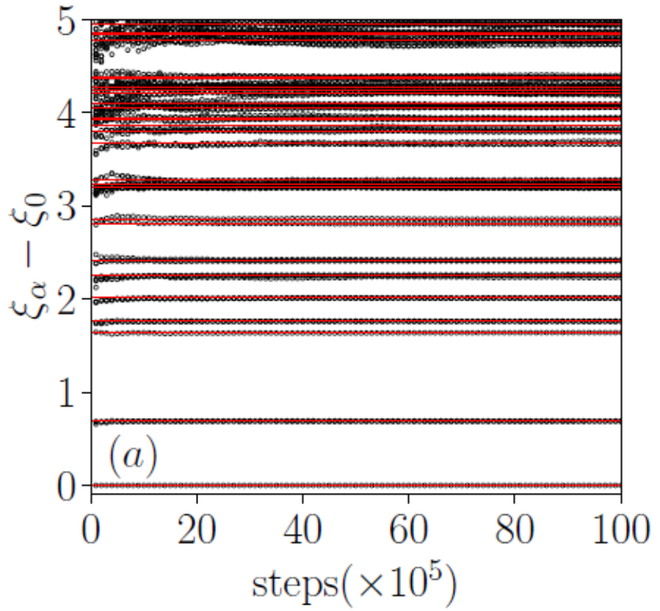
$\xi_\alpha - \xi_0$
(a)
steps($\times 10^5$)

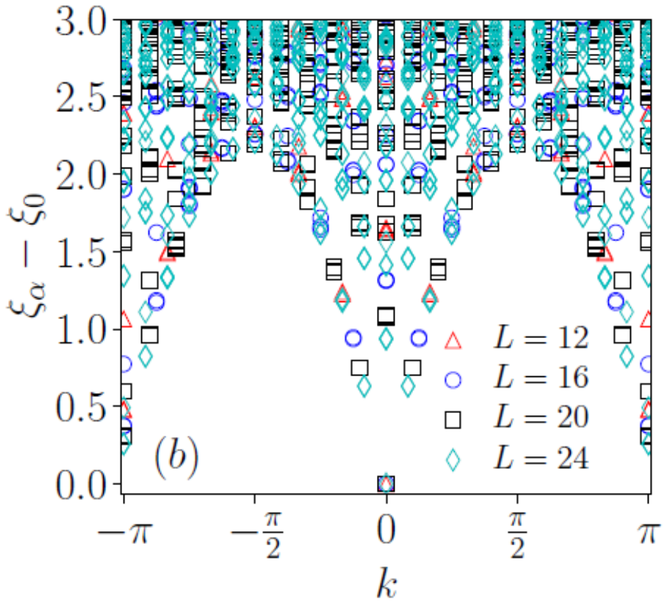
$\xi_\alpha - \xi_0$
(b)
$L = 12$
$L = 16$
$L = 20$
$L = 24$
k

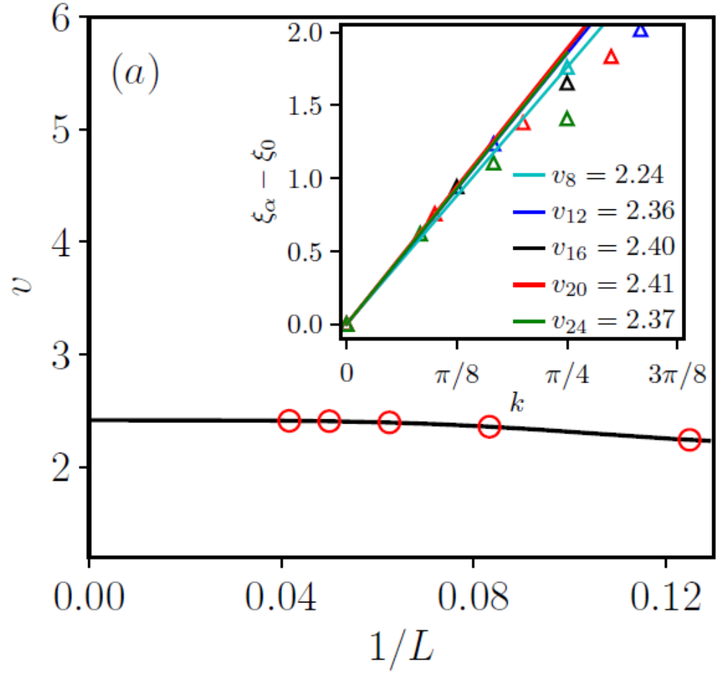
(a)
v
$\xi_\alpha - \xi_0$
$v_8 = 2.24$
$v_{12} = 2.36$
$v_{16} = 2.40$
$v_{20} = 2.41$
$v_{24} = 2.37$
k
$1/L$

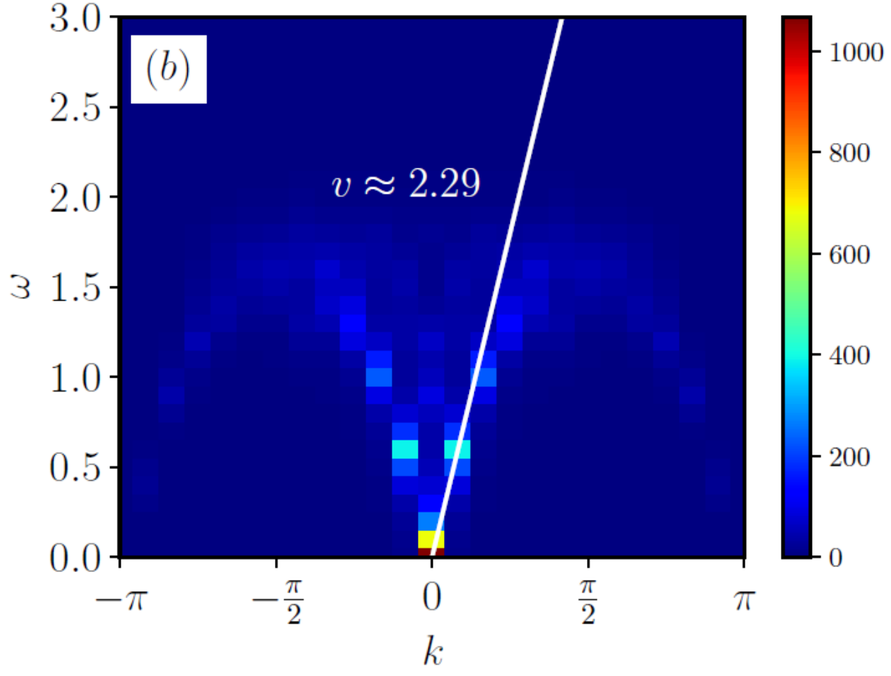
(b)
$v \approx 2.29$
ω
k

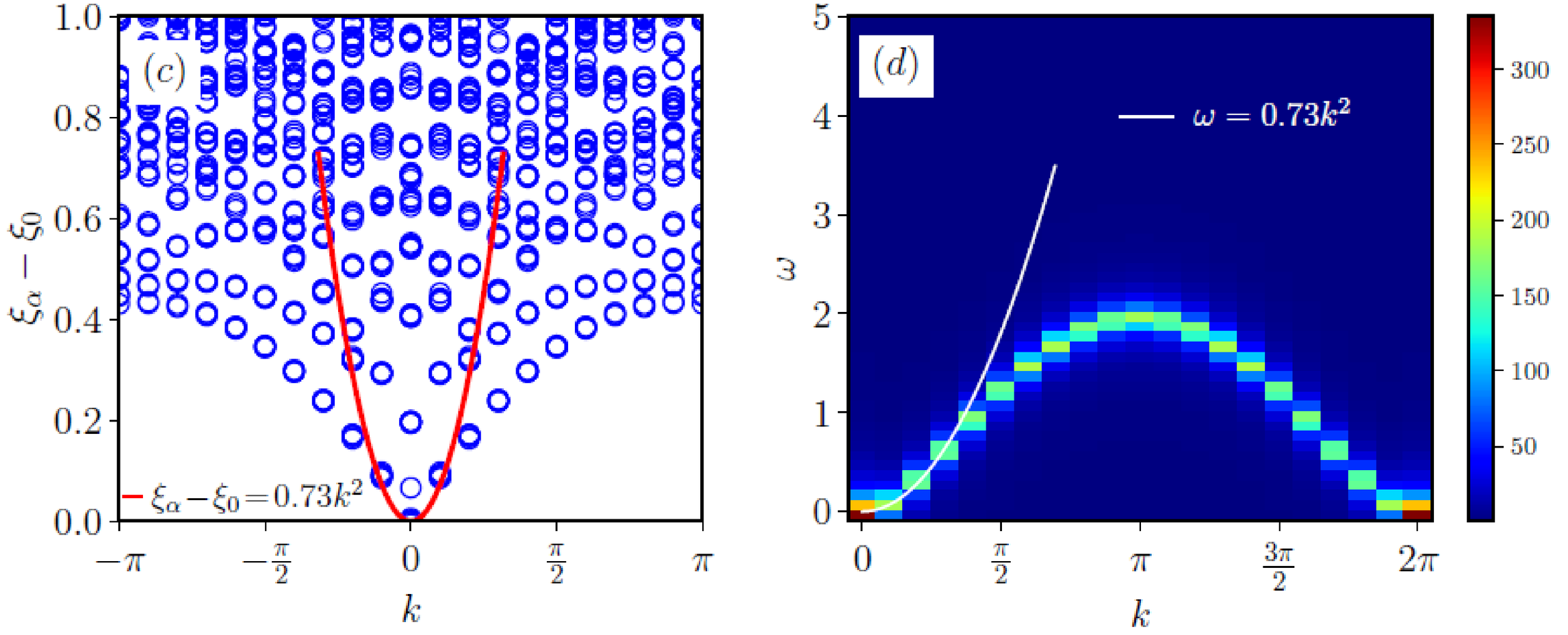
(c)
$\xi_\alpha - \xi_0 = 0.73k^2$
$\xi_\alpha - \xi_0$
k
(d)
$\omega = 0.73k^2$
ω
k

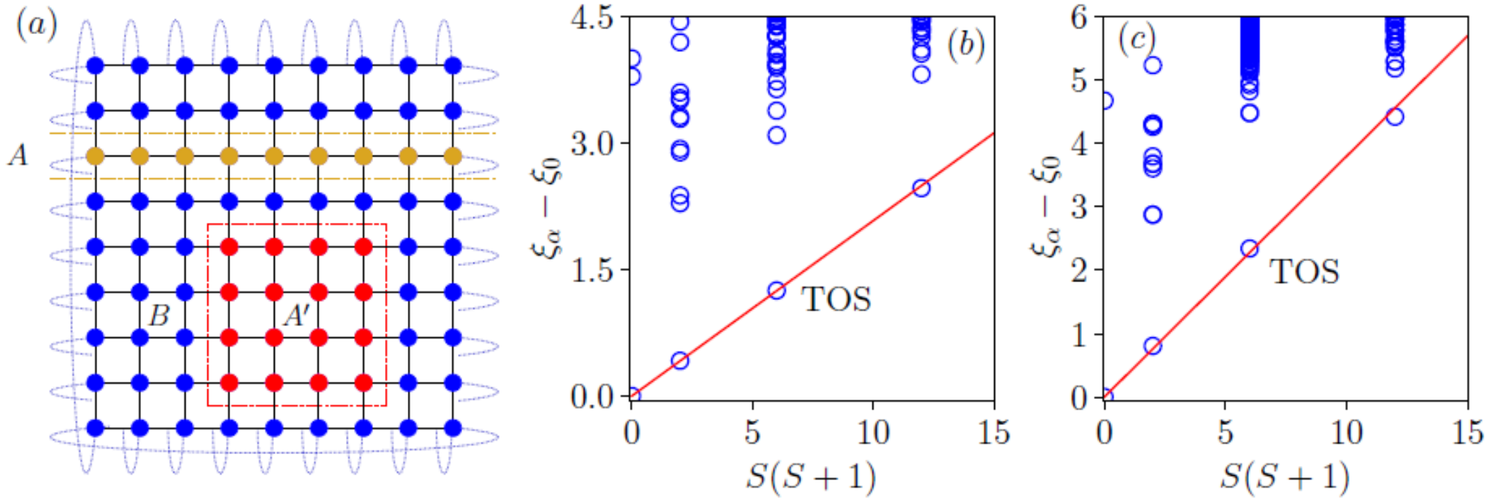

FIG. 4. (a) The AFM Heisenberg model on the square lattice. The dashed lines are used to illustrate the bipartition into two subsystems. The yellow dashed lines illustrate the cutting method that A is a ring and the red dashed lines illustrate the method that A' is a block. For each cutting method, the other part is denoted as B. We consider the square lattice model with size 20×20. We show the entanglement spectrum of EH corresponding to (b) A with length $L = 20$ and (c) A' with size 4×4. The TOS levels are connected by a red line. All the data are calculated in the total $S^z = 0$ sector.

$$E_S(L) - E_0(L) = \frac{S(S+N-2)}{2\chi_\perp L^d}$$

$\chi_\perp \sim 0.08$. The $\chi_\perp$ here is basically consistent with the QMC result (~ 0.07 [77]) of square lattice AFM Heisenberg model in thermaldynamic limit obtained through size extrapolation [81].

Z. Deng, L. Liu, W. Guo, and H. Q. Lin, Phys. Rev. B 108, 125144 (2023).

Thanks for your attention!

Positions of Postdoc & PhD students are open!

Welcome to our group and Hangzhou!

Homepage: https://zheng-yan-group.github.io/